THE EFFECT OF SMALL ADDITIONS OF TITANIUM ON THE INCUBATION PERIOD OF ISOTHERMALLY TRANSFORMED ZIRCONIUM-NIOBIUM ALLOY

by

NEE ATTOH VANDERPUYE

A THESIS SUBMITTED IN PARTIAL FULFILMENT OF
THE REQUIREMENTS FOR THE DEGREE OF
MASTER OF APPLIED SCIENCE
in the Department
of
MINING AND METALLURGY

We accept this thesis as conforming to the standard required from candidates for the degree of MASTER OF APPLIED SCIENCE

Members of the Department of
Mining and Metallurgy

THE UNIVERSITY OF BRITISH COLUMBIA
September, 1958.

ABSTRACT

The general effect of small additions of titanium on the incubation period preceding the $\beta \rightarrow \alpha + \beta$ reaction in an isothermally transformed zirconium - 17.6% niobium alloy has been studied by observing electrical resistance at constant temperature, by making micro-hardness tests, by examining specimens metallographically and by employing X-ray diffraction methods.

It was found that the effect of increasing the amount of titanium was to lengthen the incubation period. According to the electrical resistance data, an alloy containing 5% titanium shows an incubation period of approximately 15 minutes while one containing 15% titanium shows a period of approximately 25 minutes at 600°C. Micro-hardness tests show the same general effect; however, corresponding incubation periods for the same alloys are approximately 30 minutes and 40 minutes. Although metallographic and X-ray diffraction results did not conflict with these conclusions, it has been pointed out that more data and some refinement in technique are needed in order that these might be employed to support resistance data with confidence. The presence of a hydride phase in quenched and partially transformed specimens was noted. The effect of this phase on the mode and rate of reaction is unknown. Clearly, further investigation is necessary if its effect on the transformation must be determined.

It has, however, been shown that the method of observing transformations in this system with electrical resistance is both effective and sound.

In presenting this thesis in partial fulfilment of the requirements for an advanced degree at the University of British Columbia, I agree that the Library shall make it freely available for reference and study. I further agree that permission for extensive copying of this thesis for scholarly purposes may be granted by the Head of my Department or by his representative. It is understood that copying or publication of this thesis for financial gain shall not be allowed without my written permission.

Department of Mining and Metallurgy

The University of British Columbia,
Vancouver 8, Canada.

Date Nov. 7, 1958.

ACKNOWLEDGEMENT

The author is grateful for financial aid in the form of a research assistantship provided by the Defence Research Board of Canada under Research Grant DRB 7510-18.

The author would like to thank Dr. Barrie of the Physics Department most humbly for his help in the analyses work and for showing untiring interest in the investigation generally.

Many thanks to Mr. R. Butters and Mr. R. Richter for the invaluable technical advice and assistance they rendered. Finally, the author is most indebted to Dr. V. Griffiths under whose direction this investigation was performed.

TABLE OF CONTENTS

Table of Contents (Cont'd.)

LIST OF ILLUSTRATIONS

FIGURE PAGE

LIST OF TABLES

THE EFFECT OF SMALL ADDITIONS OF TITANIUM ON THE INCUBATION PERIOD OF ISOTHERMALLY TRANSFORMED ZIRCONIUM-NIOBIUM ALLOY

I. INTRODUCTION

Purpose

Comprehensive experimental programmes undertaken to develop zirconium aim at fulfilling two objectives: firstly, to enlarge the theory and knowledge of the metallic state; secondly and perhaps of more immediate import is the development of suitable alloys for industrial use. It is the purpose of this investigation to add to the general data on zirconium by studying the effect of small additions of titanium on the incubation period of an isothermally transformed zirconium-rich niobium alloy. Specifically, it complements an isothermal transformation study of a zirconium-niobium alloy conducted by Finlayson[1] and work on the constitutional diagram of a zirconium-niobium-titanium ternary recently completed by Whitmore.[2]

The nature and history of the studies on zirconium and zirconium alloys have been dealt with by Lustman[3] and Kerze. Recently a critical review of the alloying behaviour of the metal has been published by Pfeil.[4] Pfeil has also treated the theoretical aspects of the alloying behaviour of zirconium in another report.[5] The most extensive application of zirconium in industry is in certain types of nuclear reactors where the low absorption cross section for thermal neutrons is the chief cited property of the metal. Niobium, like zirconium, has useful properties applicable to reactor design. Lately, interest in ternary alloys has grown owing to their success in meeting certain operating requirements in some nuclear reactors.

The Incubation Period and Isothermal Transformation

Zirconium exhibits allotropy. The low temperature modification, a close packed hexagonal structure, is stable below 862°C. Above this temperature and up to the melting point, 1860°C, the stable phase, beta, possesses a body-centered cubic sturcture. It has been established[3] that if pure zirconium is homogenized above the transition temperature and then quenched, it is impossible to retain the beta phase. However, the addition of a second element makes retention of the beta phase possible but in varying degrees depending upon the element and the amount present. The degree of retention is shown by the sluggishness of the forward reaction ($\beta \rightarrow \alpha + \beta$). The length of the incubation period which precedes the reaction is a measure of the sluggishness of the reaction. The isothermal studies of Domagala[6] on Zr-Nb alloys, of Domagala[7] and coworkers on Zr-Mo alloys, and finally of Finlayson[1] on Zr-16% Nb alloy all show incubation periods preceding the start of transformation. Figures 1, 2, 3, and 4 show the isothermal diagrams (or Time Temperature Transformation charts) of Domagala, Finalyson, Domagala and coworkers. These diagrams are based upon electrical resistance data. Of the two zirconium-niobium alloys investigated by Domagala, only one chart representing the 7% niobium alloy is shown here. However, a quick study of electrical resistance data for the 15% niobium alloy clearly reveals the effect of additions of niobium upon the incubation period. The incubation period for the 15% alloy is greater than that for 7% alloy. The two charts[7] of the zirconium-molybdenum system, (Figures 3 and 4) together with two others not reproduced here, also show that increasing amounts of molybdenum lengthen the incubation period. At 600°C, the incubation periods preceding the $\beta \rightarrow \alpha + \beta$ reaction are half a minute and two minutes for 5.4% and 7.5% Mo alloys respectively.

The transformation requires that a nucleus of the new phase must form

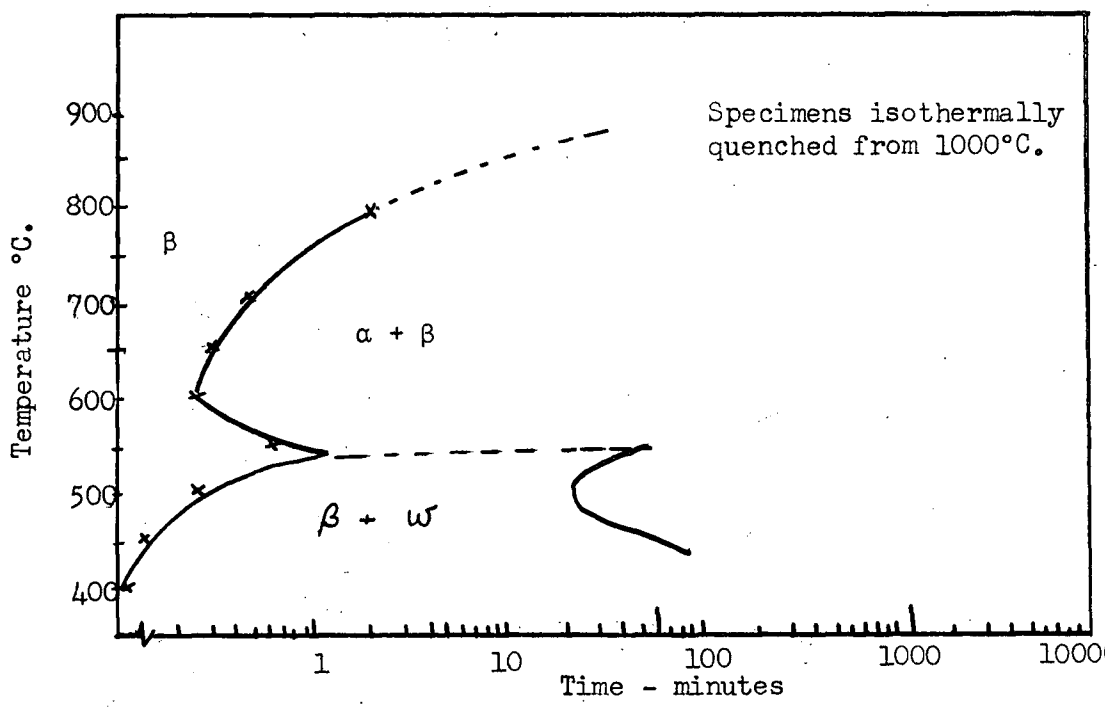

Figure 1. T-T-T chart for a Zr-7% Nb alloy (after Domagala[6])

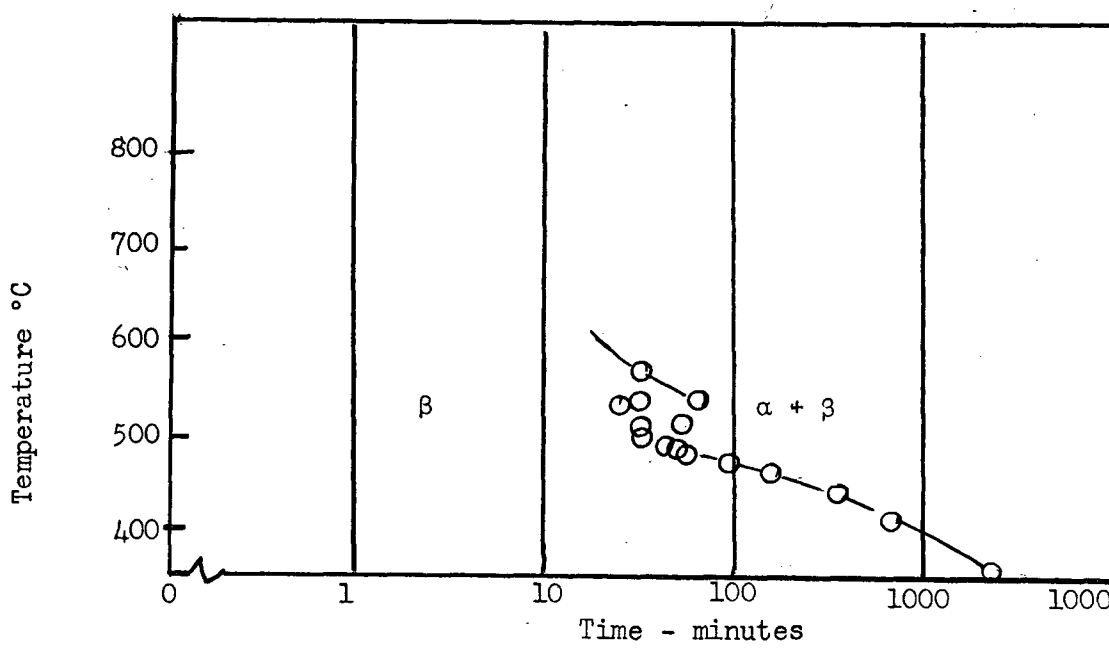

Figure 2. Tentative T-T-T chart for Zr-16.4% Nb alloy (after Finlayson[1]).

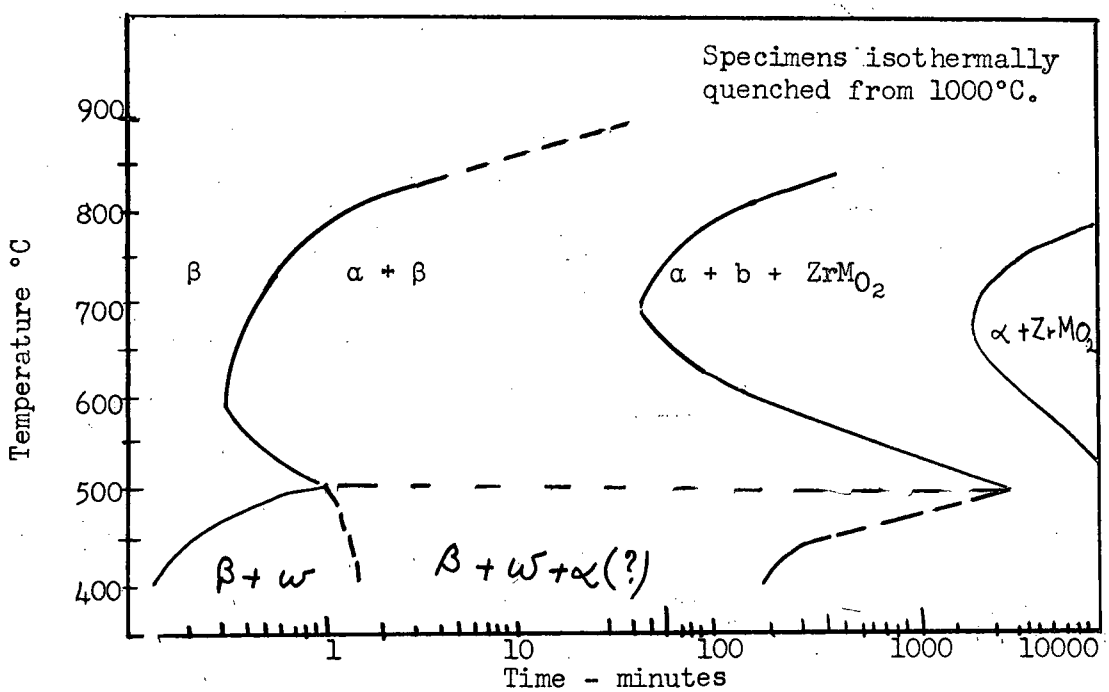

Figure 3. T-T-T chart for Zr-5.4% Mo alloy (after Domagala and coworkers[7]).

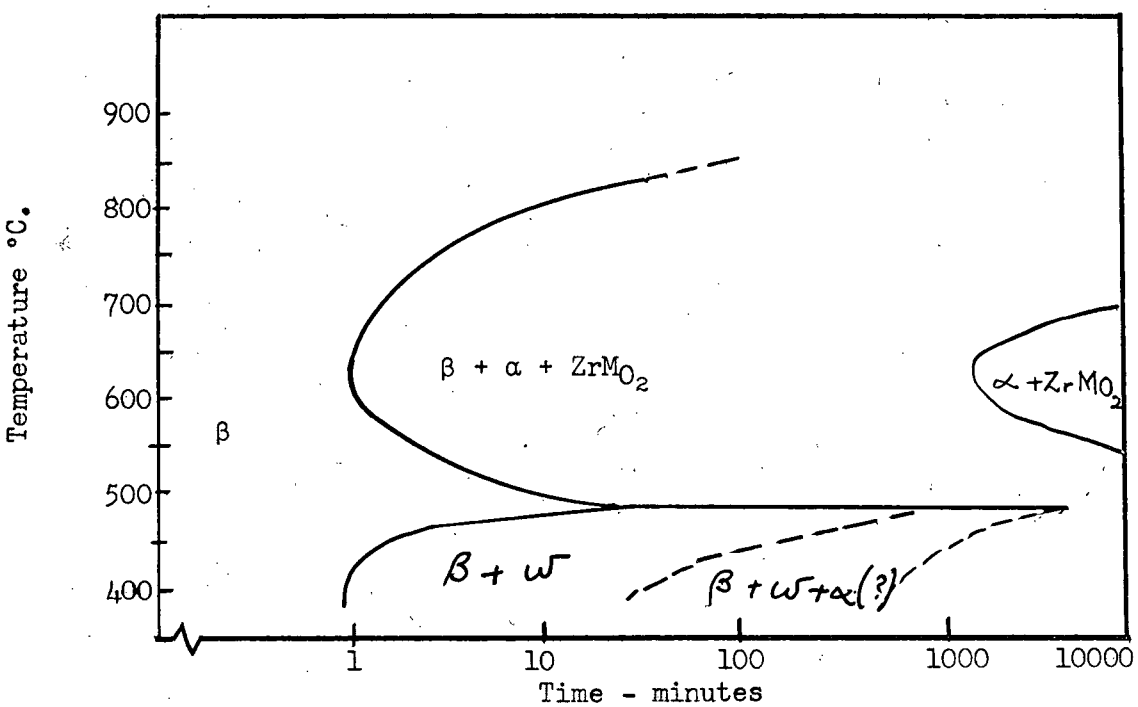

Figure 4. T-T-T chart for Zr-7.5% Mo alloy (after Domagala and coworkers[7])

and reach a critical size before the growth of the nucleus can be assured. Apparently the incubation period is the time it takes to nucleate the transformation. The whole process of nucleation and subsequent transformation is controlled by composition fluctuations and diffusion of the atoms involved. It is generally believed that the rate of diffusion of atoms during such transformations is decreased by impurities. Thus it can be understood why alloy additions generally have the effect of increasing the incubation period. At high temperatures the vibrational frequency of atoms is high and consequently the probability of destruction of nuclei of the new phase is equal to that of formation. At low temperatures, the rate of diffusion is much lower; hence the probability of formation of these nuclei is also small. It may be assumed, therefore, that some intermediate temperature range offers the optimum opportunity for the formation and subsequent growth of nuclei of the new phase. If the probability for the reaction taking place bears any relation to the incubation time, then the general nature of the incubation time versus temperature curve should be a 'C' with at least one minimum in the time ordinate at some intermediate temperature. Thus the length of the incubation period is a function of temperature as well as the type and amount of impurity present.

The transformation represents an irreversible reaction in which the stable product is first nucleated and then grown at the expense of the reactant phase. In constitutional studies, equilibrium conditions are maintained. However, subcooling, such as practised in this investigation, represents marked departure from equilibrium cooling. The reaction thus may produce intermediate products as well as stable ones. Figures 1, 3, and 4 show an w phase that is not evident in the constitutional diagrams of zirconium-niobium and zirconium-molybdenum systems. A literature search revealed that several general analyses have been made of the isothermal transformation itself and not of the incubation

period. These show the nature of the time-dependence. Austin and Rickett[8] set the fraction transformed as:

$$\alpha = K_1 (1 - \alpha)t^p \qquad (1)$$

where K_1 and p are constants. The rate of reaction was given by T. Mishima, Hasiguti and Kimura[9] as:

$$\frac{d\alpha}{dt} = K_2\alpha^{(p-1)} (1 - \alpha)^{(p+1)/P} \qquad (2)$$

An approach more generally used is to take the right hand side of the equation (1) as the rate of transformation and:

$$\frac{d\alpha}{dt} = K (1 - \alpha)t^{m-1} \qquad (3)$$

Integration gives:

$$\alpha = 1\text{-}\exp\left[-K_4 t^m\right]$$

$$= 1\text{-}\exp\left[-\left(\frac{t}{\tau}\right)^m\right] \qquad (4)$$

with $K = K_{3/m} = \tau^{-m}$

where τ is a time constant.

The Zirconium-Niobium System.

Pfeil[5] and Smoluchowski[3] have discussed the theoretical aspects of the alloying behaviour of zirconium, while McIntosh[10] has reviewed the alloy systems of niobium. Literature search revealed that actual experimental work on the zirconium-niobium system was first performed by Anderson and coworkers at the U.S. Bureau of Mines.[11] Their results showed that it is indeed difficult to retain beta in pure zirconium, for of the three alloys prepared, 0.6%*, 5.1% and 12.9%, increasing amounts of beta were retained as the niobium content grew larger. The alpha phase was described as Widmanstatten structure in the 0.6%

* All compositions, unless otherwise stated, are in weight percent.

alloy. The fact that the 12.9% alloy showed much larger grains indicated that the beta → alpha transformation took place at a relatively low temperature. Clearly the transformation temperature is depressed by alloying with niobium. In general, simple substitutional alloying will produce a stronger material by virtue of the induced lattice strain. Simcoe[12] and Mudge observed an increase in strength in both 0.5% and 1.0% niobium alloys made with hafnium-containing zirconium. According to Keeler,[13] the strength of zirconium is increased by additions of niobium to a content of at least 3%. This general strengthening effect is borne out in part by the results of Anderson[13] and Litton[14] which are reproduced in Finlayson's report. If it is assumed that the beta structure is weaker than the alpha, then a second effect such as the sluggishness of the transformation caused by the addition of some element or by heat treatment may, by inducing large amounts of beta to be present, render the final material to be weaker than would be expected from substitution alone. Thus the difference between the yield strength values of Litton and those of Anderson was probably due to inconsistent heat-treating.

In 1952 Hodge[15] investigated the zirconium system up to 25% niobium. He suggested tentatively that the eutectoid in the zirconium-rich alloys lay at about 625°C and 10% niobium and estimated that the solubility of niobium in zirconium at 625°C was near 6%.

The constitutional diagram of Rogers and Atkins[16] published in 1955 is shown in Figure 5. Solubility in alpha zirconium reaches a limit at about 6.5%. The system thus shows age-hardening effects. The iodide zirconium employed by Rogers and Atkins contained traces of hafnium (less than 0.05%). The chief impurities in the niobium were tantalum (0.5%) and traces of iron, silicon and titanium.

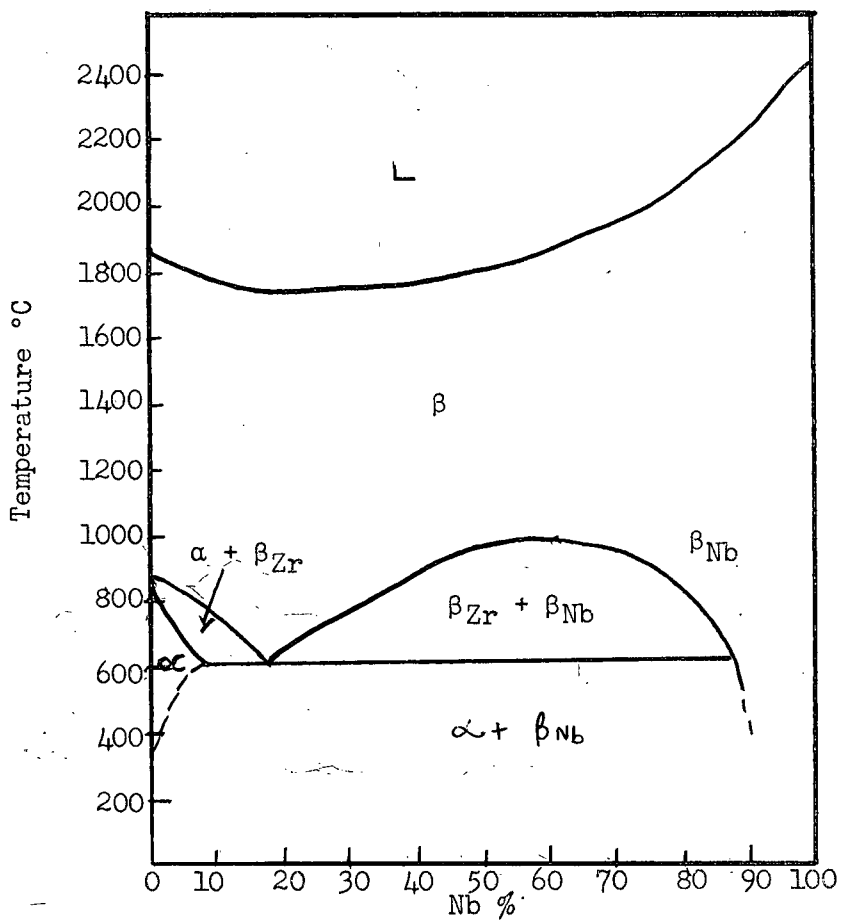

Figure 5. The zirconium-niobium phase diagram (after Rogers and Atkins)

In 1956, Domagala and McPherson[17] reported their investigation of the zirconium-niobium system. Although they used iodide zirconium and 'high purity' niobium powder, they agreed with Rogers and Atkins only in part. For they put the eutectoid horizontal at 800°C, the eutectoid composition at 17% niobium and maintained that a continuous series of solid solutions existed only above 1180°C.

Again, in 1957, Bychkov[18] and coworkers presented a phase diagram that was inconsistent with that of Rogers and Atkins. Their eutectoid horizontal was at 550°C and the eutectoid composition at 12% niobium. Furthermore, the minimum in the solidus was at 1600°C rather than at 1740°C as found by Rogers and Atkins.

Composition of Ternary Investigated

The addition of titanium to a zirconium-niobium alloy results in a ternary. In order to appreciate the ternary diagram, the two other binaries, Zr-Ti and Ti-Nb, are shown in Appendix A. The diagram Zr-Ti shown is that of Fast[19] with slight modifications by Hayes et al.[20] That representing titanium-niobium was determined by Hansen[21] et al. From Whitmore's investigation of the zirconium-rich side of the zirconium-niobium-titanium ternary, five isothermals are presented in Figures 6, 7, 8, 9 and 10. These are isothermals at 800°C, 700°C, 650°C, 600°C and 550°C. If the proportion of zirconium to niobium is kept constant, then the addition of titanium may be shown easily since it will lie on a ternary isopleth.[22] The proportion of zirconium to niobium in the ternary alloy was 7:1.5 or 17.6% Nb in a zirconium-niobium alloy. Alloys containing 5% and 15% titanium (shown on the ternary isopleth in Figures 6 to 10) were investigated.

Effect of Impurities.

The system under investigation is made up of reactive metals. Consequently the nature and extent of contamination must be known. The major contaminants are oxygen, nitrogen, hydrogen and hafnium. The related binary diagrams of these impurity elements with zirconium are presented in Appendix B.

Oxygen and nitrogen raise the α/β transformation temperature making α more stable. Therefore an immediate effect of the presence of these two gases in this investigation is to affect the relative position with respect to temperature of the isothermal curve. A second and probable effect is to change the rate of reaction and thus the shape of the curve. They may introduce phases which can alter properties such as resistance and hardness. According to Schwartz and Mallett[23] the familiar needles found in the microstructure of

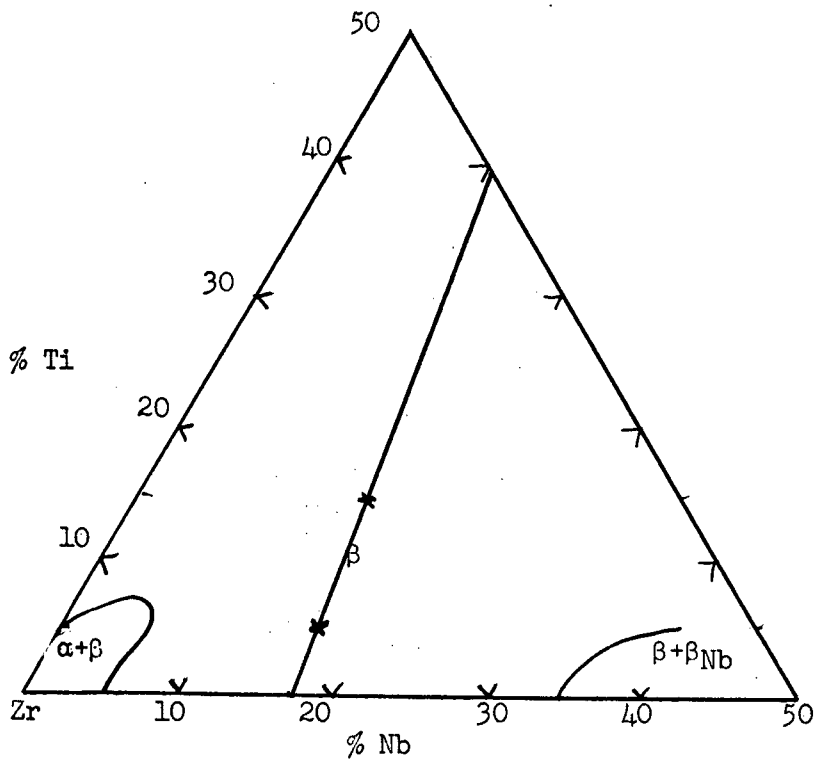

Figure 6. Isothermal section of Zr-Nb-Ti ternary at 800°C (after Whitmore[2])

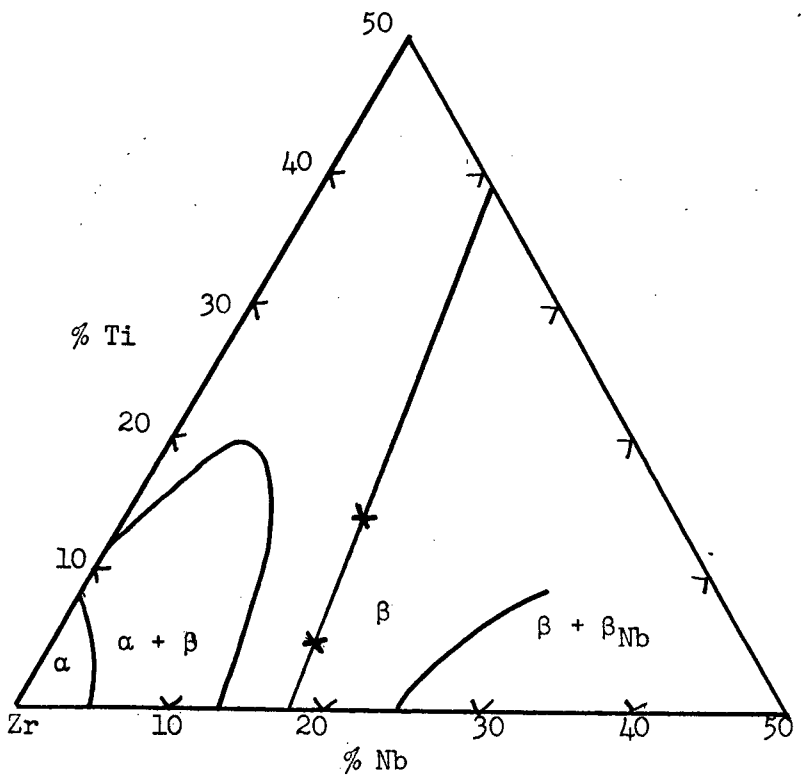

Figure 7. Isothermal sectionof Zr-Nb-Ti ternary at 700°C (after Whitmore[2])

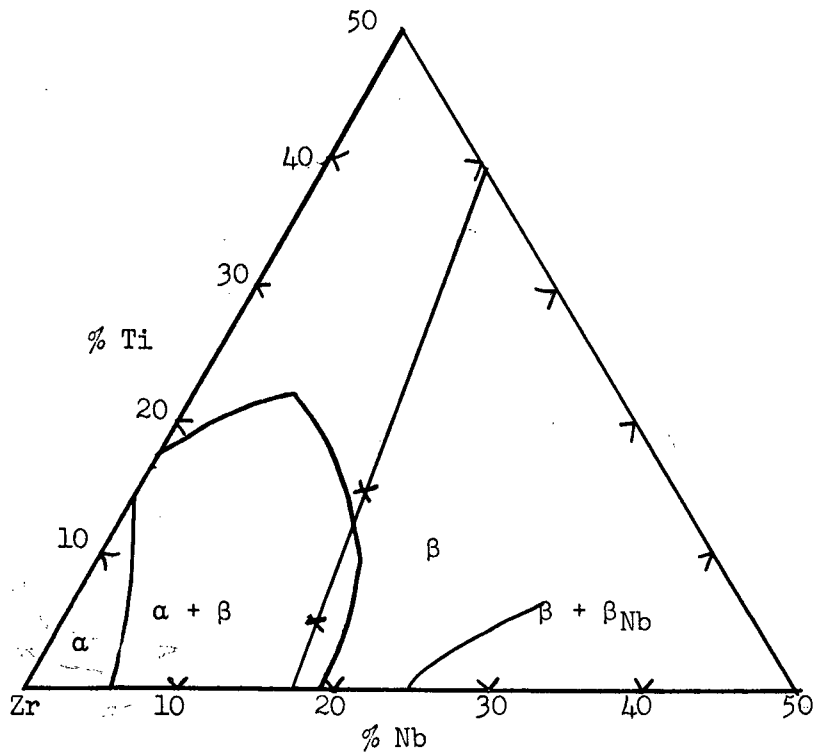

Figure 8. Isothermal section of Zr-Nb-Ti ternary at 650°C (after Whitmore[2]).

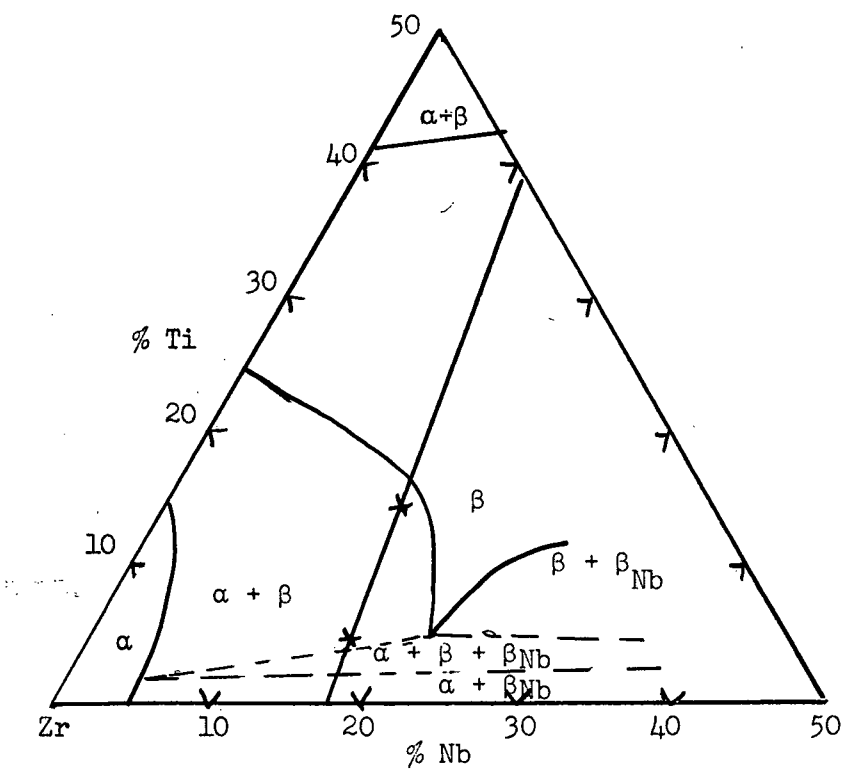

Figure 9. Isothermal section of Zr-Nb-Ti ternary at 600°C (after Whitmore[2]).

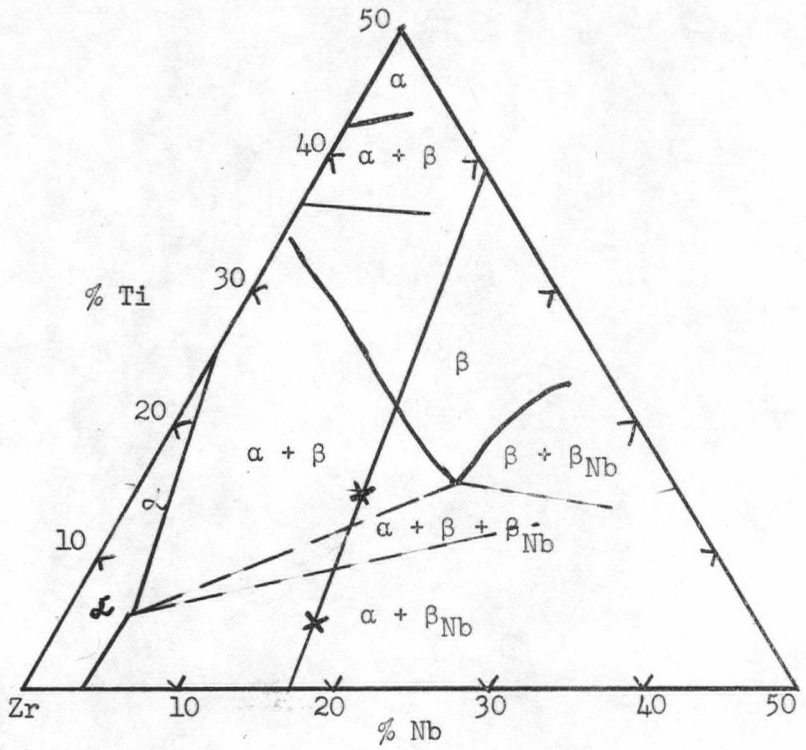

Figure 10. Isothermal section of Zr-Nb-Ti ternary at 550°C (after Whitmore)

quenched zirconium alloys represent hydride phases. Figure 11 shows these needles in a zirconium-niobium-5% titanium alloy that has been quenched from

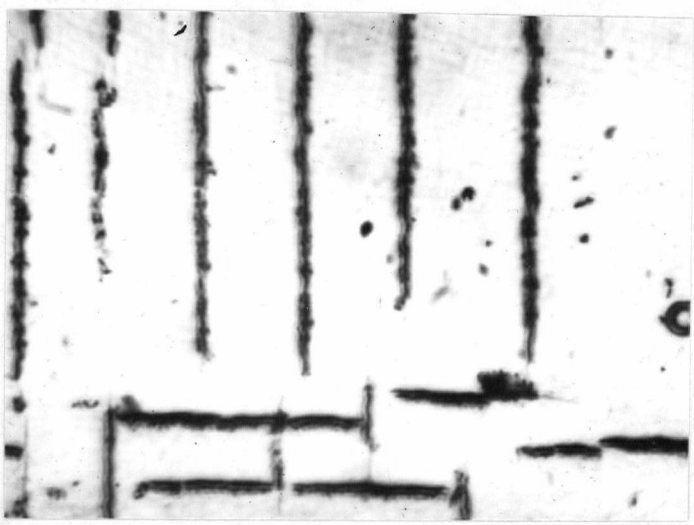

Figure 11. Quenched (5% Ti) alloy showing needles of hydride phase. Etch HF + HNO_3 + Lactic acid, X 1500.

900°C. While contamination by these gases cannot be entirely eliminated, it may be minimised only when the best high-vacuum or inert atmosphere techniques are employed. These gases are so stable in zirconium, niobium and titanium that removal in their elemental form at practical temperatures and pressures is difficult.

The presence of hafnium is not thought to have any serious effects since it is completely soluble in zirconium. Thus iodide zirconium which contains more hafnium and less oxygen than sponge zirconium is more desirable in this investigation.

Techniques for Studying Transformations.

Given a reaction involving reactants and products, it is possible to distinguish between these because of the difference in properties. In choosing some property to show the nature and rate of the reaction, the fundamental quality is the direct relation between the amount of the property and the amount of reactant or product present. Cottrell[24] calls these properties 'capacity properites' in contrast to properties such as density or resistivity which do not change as far as a component in the bulk is concerned. Broadly, capacity properties employed to show transformation may be divided into five classes:

a) Electrical - in which resistance* may be measured.

b) Magnetic - susceptibility

c) Optical - reflectivity, metallographic examination

d) Mechanical - elastic constants (dilatometric), microhardness measurements.

e) X-ray diffraction.

---

* That electrical resistance is a capacity property is shown by the analysis in Appendix CI. Resistance is a capacity property but resistivity is not.

For most metallic systems perhaps the electrical, magnetic and X-ray techniques are the most sensitive. However, the metals and conditions of experiment may impose restrictions upon choice of technique. For example, the choice of the electrical method with the given circuit assumes that the specimen can be successfully drawn into a wire. In this investigation, the electrical resistance was chosen as the main technique. To support resistance data, metallographic, mechanical (micro-hardness tests) and X-ray diffraction techniques were used.

II. EXPERIMENTAL

1. Alloy Preparation

The zirconium metal was part of a stock of iodide crystal bar produced by Foote Mineral Company. The reported analysis is given in Table 1.

Table 1.

Analysis of Crystal Bar Zirconium.

Element	Weight Percent
Hf	2.17
Si	0.005
Al	0.002
Mn	0.001
Mg	0.002
Fe	0.002
Cr	0.001
Ti	0.006
Ni	trace
Ca	0.003
Cu	0.0005
O_2	0.01

The titanium crystal bar produced by the iodide process was supplied by A.D. McKay Company. In the absence of specific analysis, a typical analysis such as quoted by McQuillan[25] may prove useful.

Table 2.

Typical Analysis of Crystal Bar Titanium.

Element	Weight Percent
O_2	0.01
N_2	0.005
C	0.03
Fe	0.04
Ca	trace
Al	0.05
Si	0.03
Pb	trace
Ni	trace
Mo	trace

Niobium rods of diameter 4.7 mm were puchased from Johnson, Matthey and Company. The accompanying spectrographic analysis is given in Table 3.

Table 3.

Spectrographic Analysis of Niobium Rod.

Element	Weight Percent
Ta	0.5
Ni	0.0007
Fe	0.004
Ti	0.012

Holes were drilled in thin slices of zirconium and titanium which had previously been sawn from the respective bars. A short rod of niobium was also sawn from the niobium rod. By careful filing and weighing, the desired proportion of each component was obtained. After cleaning with acetone, a compact mass for melting was obtained by inserting the niobium rod into the holes drilled in the other two components. The mass was then washed again in acetone.

A diagram of the levitation melting apparatus of Polonis et al[26] is shown in Figure 12. Although the levitation technique employed by Polonis et al was applied, significant changes were made. A coil of slightly different design was designed by Finlayson for melting zirconium alloys.

The power supply used was a 23.5 Kva Lepel valve oscillator. In order to suppress the tendency to arc during operation, there should either be a high vacuum or positive pressure. It was more convenient to obtain this condition with positive pressure using inert atmosphere. To achieve this, helium was purified by passing over activated charcoal at a pressure of 40 psig and at liquid nitrogen temperature. A positive pressure of 15 psig was found to be satisfactory.

The compact unit to be melted was suspended by means of a 0.005-inch

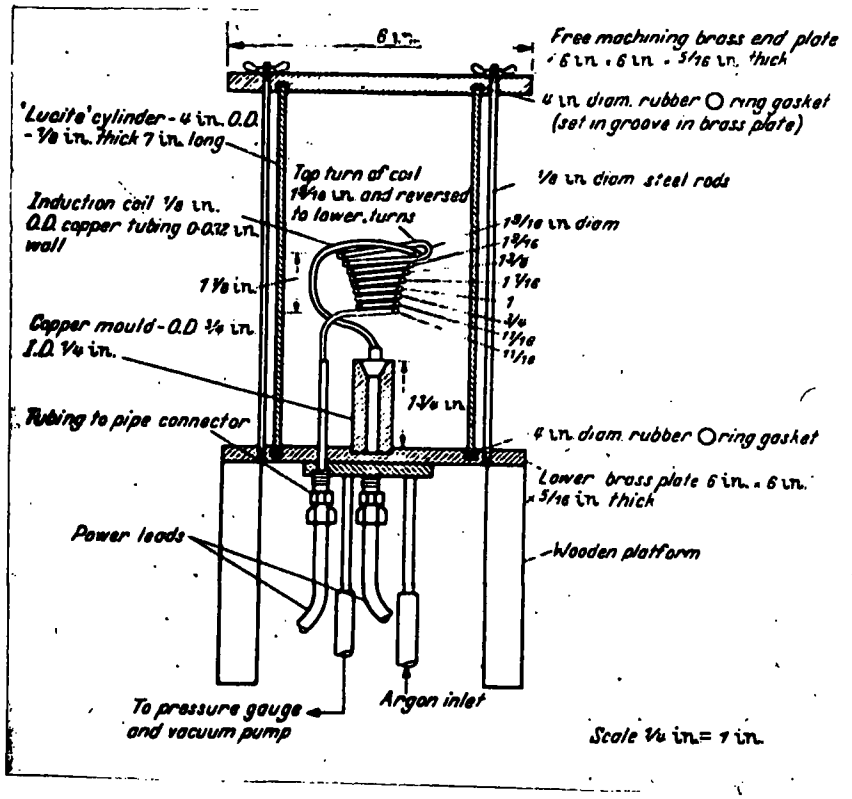

Figure 12. Diagram of the levitation melting apparatus of Polonis et al.

zirconium wire affixed to a glass rod in the roof of the chamber. After pumping for half an hour, the chamber was flushed three times with helium. The chamber was then filled to a pressure of 15 psig. Next the inert atmosphere was gettered by a hot zirconium filament of the same size as the suspension wire. Starting at 30 percent, the power was quickly turned up to 100 percent. Melting and subsequent mixing of the individual components occurred in five to ten seconds. The power was then slowly reduced to cast the ingot. A typical ingot is shown in Figure 13.

All the ingots appeared bright and clean upon removal from the copper mold. Weighing in and out gave a difference of ± 0.002 gm for a weigh-in of approximately 6.5 gm for each alloy. Apparently the amount of suspension wire involved in the alloy was negligible. It was then assumed that the weight of

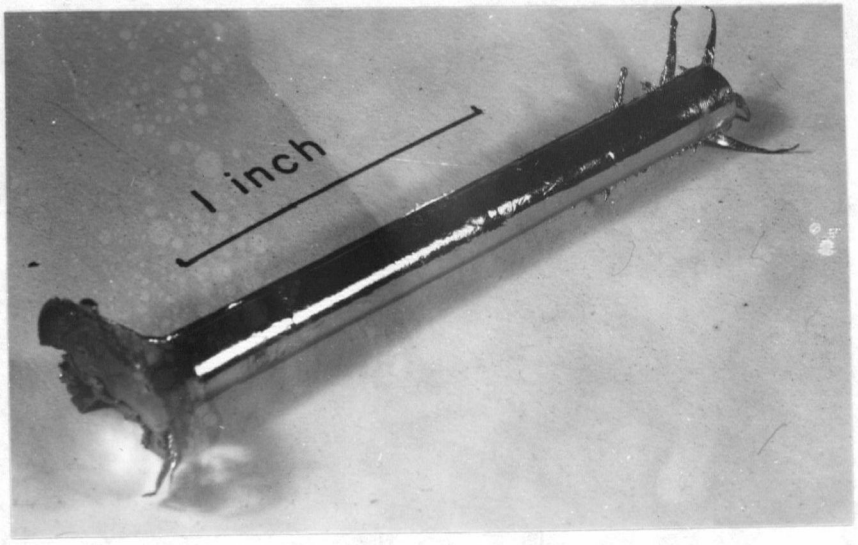

Figure 13. A typical ingot as cast by levitation melting.

each component represented the proportion in its respective alloy. The alloys were designated as Tr 1, 2, 3, i.e., Ternary 1, 2, 3. - Those actually used for the isothermal transformation presented in this report were Tr 24, Tr 25, Tr 29, and Tr 30. Tr 29 and Tr 30 contained 5% titanium while Tr 24 and Tr 25 contained 15% titanium. The proportion of zirconium to niobium in all was 7:1.5.

During the development of a suitable coil there were many unsuccessful attempts to levitate and melt batches. These attempts are represented by Tr 1 to 23. Tr 26, 27 and 28 were rejected when they failed to draw properly.

2. Resistance Measurements.

Apparatus

An apparatus was assembled to facilitate the determination of specimen resistance using the circuit of Rogers and Atkins (see Figure 14). The assembly comprised a vacuum furnace, a pumping system, a temperature control unit, a

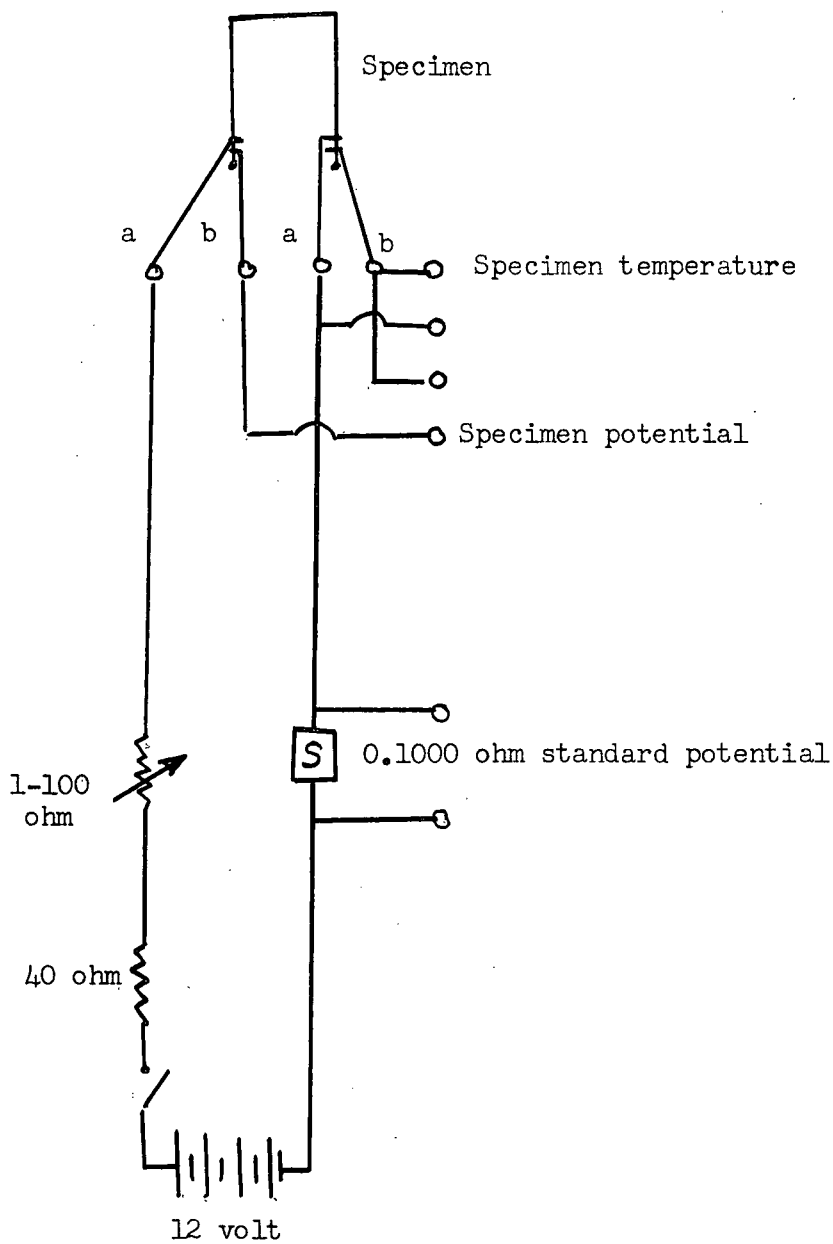

Figure 14. Diagram of resistance measuring circuit
(a) Chromel (b) Alumel

precision potentiometer and a set of lead acid cells. It is shown in Figure 15.

Minor improvements were made on the vacuum furnace designed by Finlayson (see Figures 16 and 17). Short circuiting which interrupted operations often occurred when soldering metal vaporized on to the glass-to-metal seal through which a power lead made entry into the vacuum chamber. Correction was made by inserting the seal at the end of a pipe an inch and a quarter long and thus removing it from the direct path of the metallic vapour. Another minor change was the use of a Wilson type seal through which the thermocouples passed into the chamber. Improved contact between the wire specimen and thermocouples was achieved by eliminating the clamping device employed by Finlayson. Holes were drilled with No. 78 high speed drills at the ends of 0.004-inch diameter wire specimens, the No. 28 Chromel A-Alumel thermocouples were inserted; a squeeze with suitable pliers ensured good contact. The specimen wires each 4 cm. long had been previously drawn without anneal from ingots Tr 30 and Tr 24. Two limiting factors guided the choice of the wire diameter of 0.004 inch. The length was to be sufficient for the purposes of the experiment and yet it could not be so long that its increased surface area threatened a high pick-up of oxygen and nitrogen.

The furnace windings were made with tantalum wire. Power control was achieved with a Honeywell Circular Scale Controller using a Pt-Pt 10RH thermocouple; the position of the latter is shown in Figure 17. Operating on a 220V circuit, temperatures in the furnace were controlled to $\pm 0.5°C$.

The vacuum system consisted of a mechanical fore pump, an oil diffusion pump and a liquid air trap. Vacuum pressure of better than 10^{-5} mm. Hg was achieved at operating temperatures.

The standard resistor, S, shown in Figure 14 was 0.100 ohm.

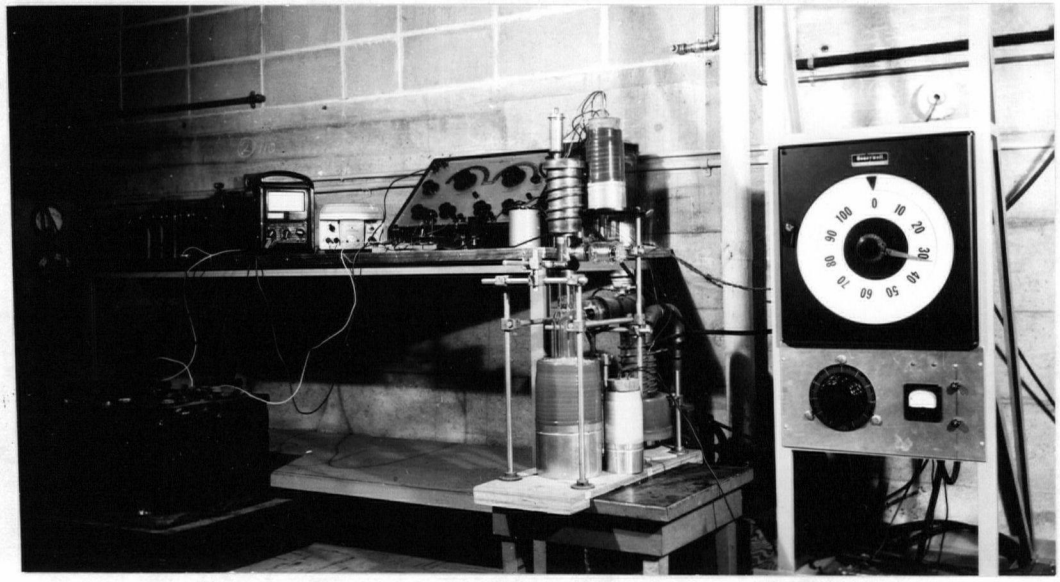

Figure 15. General view of apparatus showing furnace control unit, vacuum system, vacuum furnace, potentiometric measuring equipment. Pressure measuring apparatus is not shown.

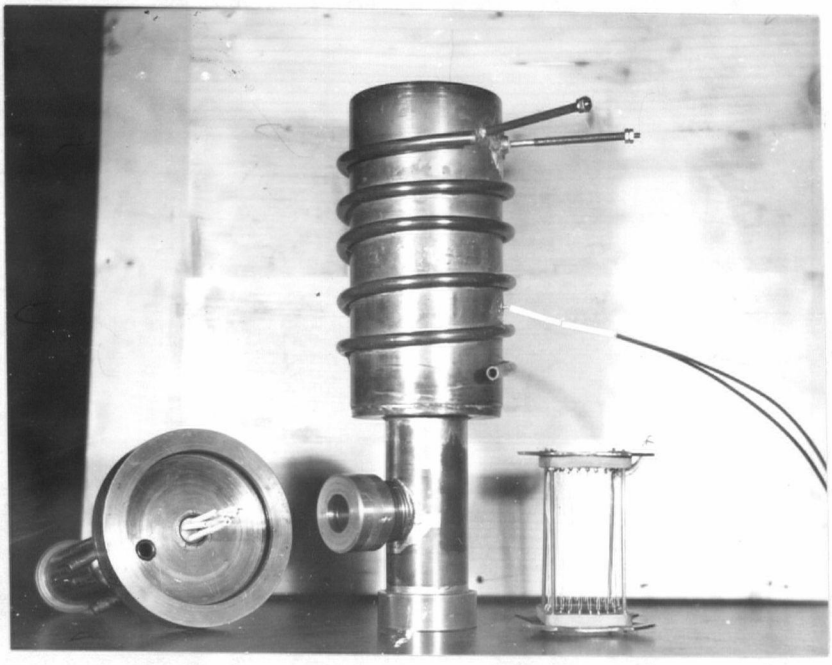

Figure 16. View of main vacuum furnace elements, water cooled can, lid showing the thermocouple.

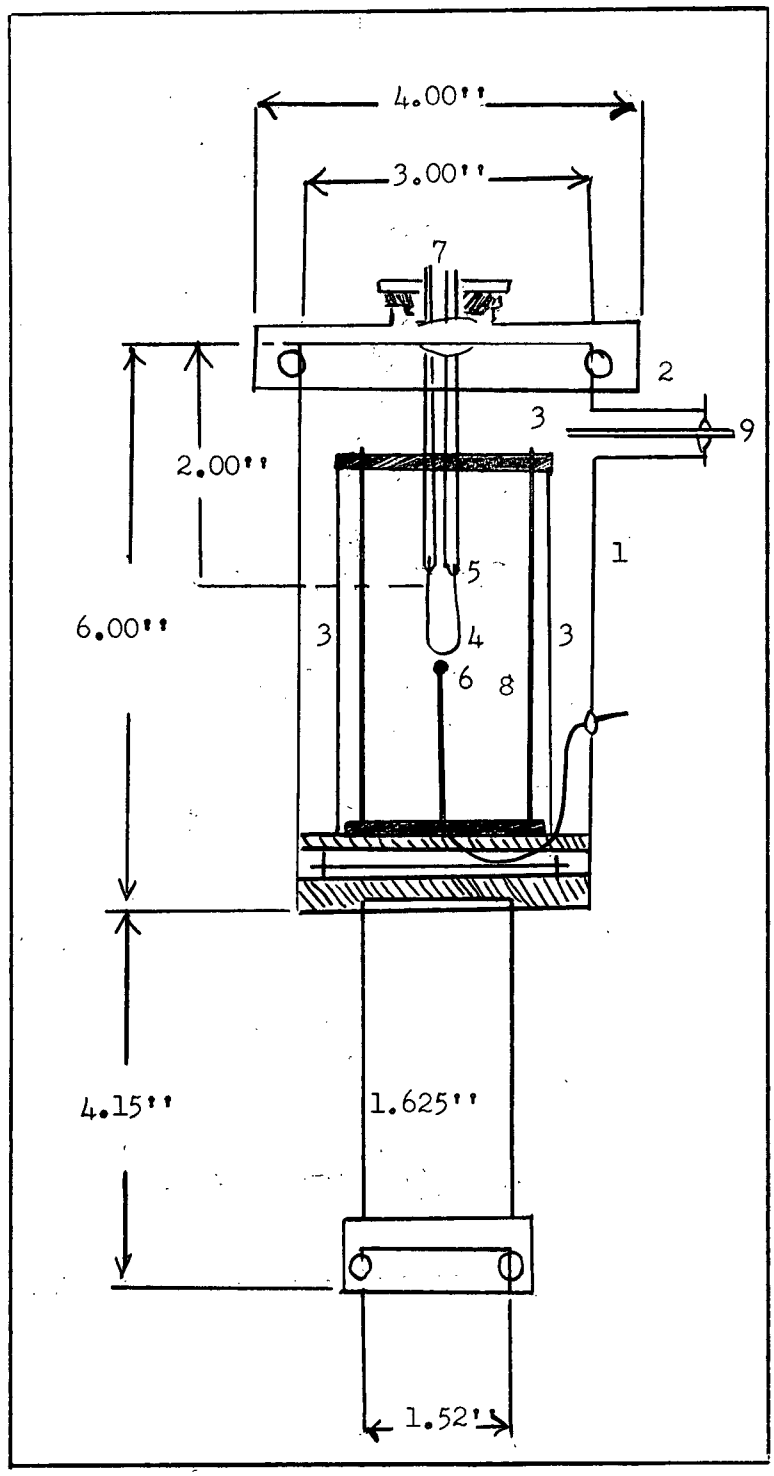

Figure 17. Diagram of Furnace and Vacuum Chamber Assembly

1. Brass can
2. Brass lid with Wilson type seal
3. Radiation shields
4. Specimen
5. Specimen-thermocouple contact
6. Furnace control thermocouple
7. Measuring thermocouples.
8. Self-gettering furnace.
9. Power lead through glass-to-metal seal.

Potenials were measured on a Pye Precision Potentiometer in conjunction with a Pye Scalamp Galvanometer. Employing Ohm's law, if a constant current is maintained, then changes in potential are proportional to changes in resistance. Thus if the connections are made as shown in the circuit diagram (Figure 14), the potential of the specimen may be measured at a selected temperature.

Procedure

In order to obtain a homogeneous beta structure, specimens were heated to 900°C for one hour. The furnace power was then reduced so as to bring the specimen to the desired transformation temperature. This temperature was reached in 60 seconds or less. The specimen was then maintained at this temperature for several hours after which it was quenched to room temperature by shutting off the power. A new specimen was inserted and the procedure was repeated for yet a lower transformation temperature. Runs were accomplished for 800°C, 700°C, 600°C, 500°C, 400°C and 300°C. During the time when the specimens were held at the above mentioned temperatures, simultaneous readings of potential and temperature were observed. To read the potential a steady current (68 ma, 70 ma, or more) was passed through the specimen with the aid of a variable resistance unit. A temperature reading followed immediately with no current passing through.

Results and discussion.

The 'potentials' data and calculated resistances are tabulated in Appendix D. Figures 19 and 20 show the plot of resistance vs time for Tr 30 and Tr 24. Figure 18 shows the plot of resistance vs temperature during slow heating of a 5% Ti alloy. Tentative partial isothermal transformation plots delineating the start of transformation in the two alloys are shown in Figure 21. The data show that transformation starts at some temperature much below 800°C. After an incubation period, the body-centered phase begins to transform

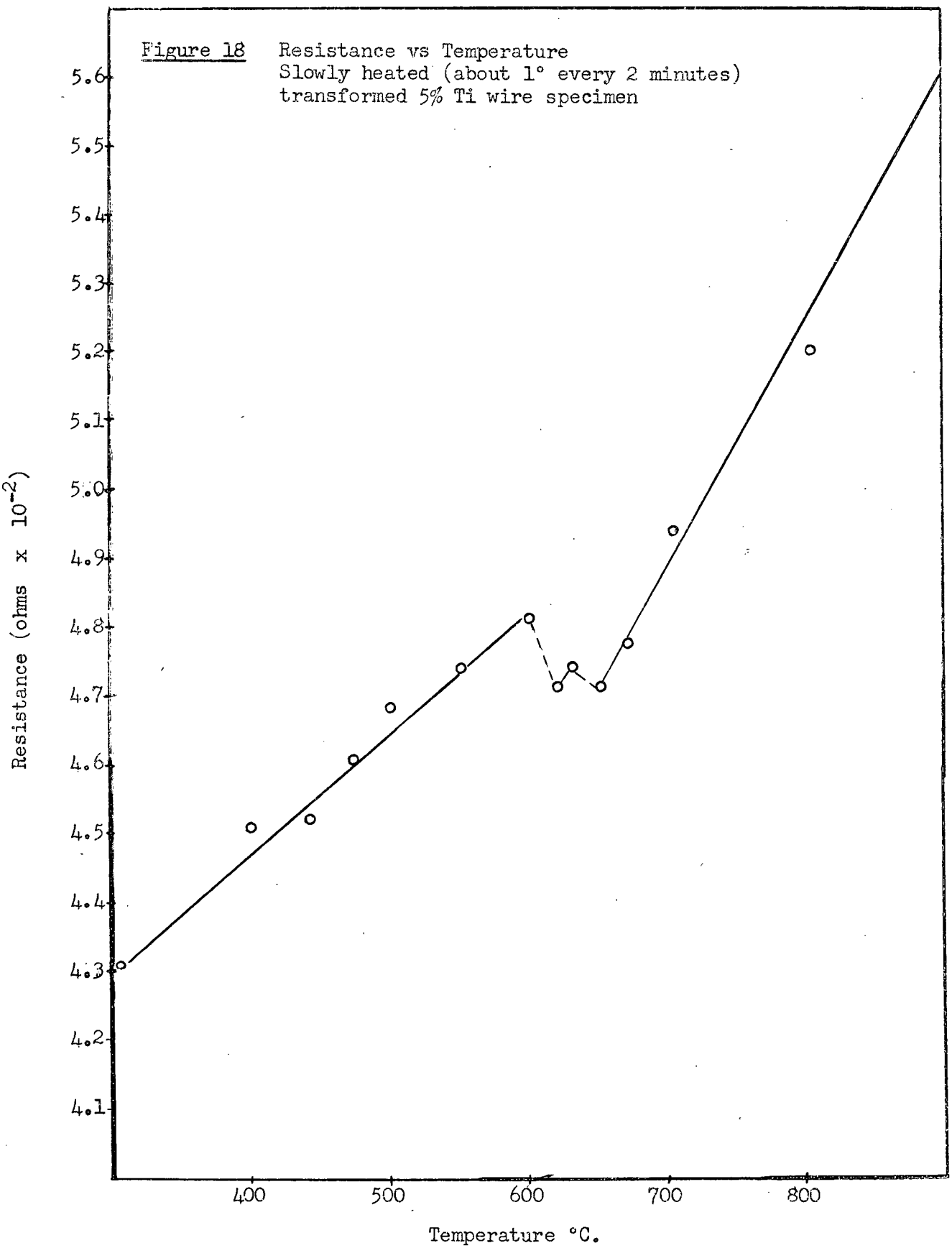
Figure 18 Resistance vs Temperature
Slowly heated (about 1° every 2 minutes)
transformed 5% Ti wire specimen
Resistance (ohms x 10^{-2})
5.6
5.5
5.4
5.3
5.2
5.1
5.0
4.9
4.8
4.7
4.6
4.5
4.4
4.3
4.2
4.1
400
500
600
700
800
Temperature °C.

Figure 19a Resistance vs Time
Tr 30 Composition Zr:Nb = 7:1.5 Ti = 5% of total weight
Specimen homogenized at 900°C for 1 hour
Quenched to temperature indicated

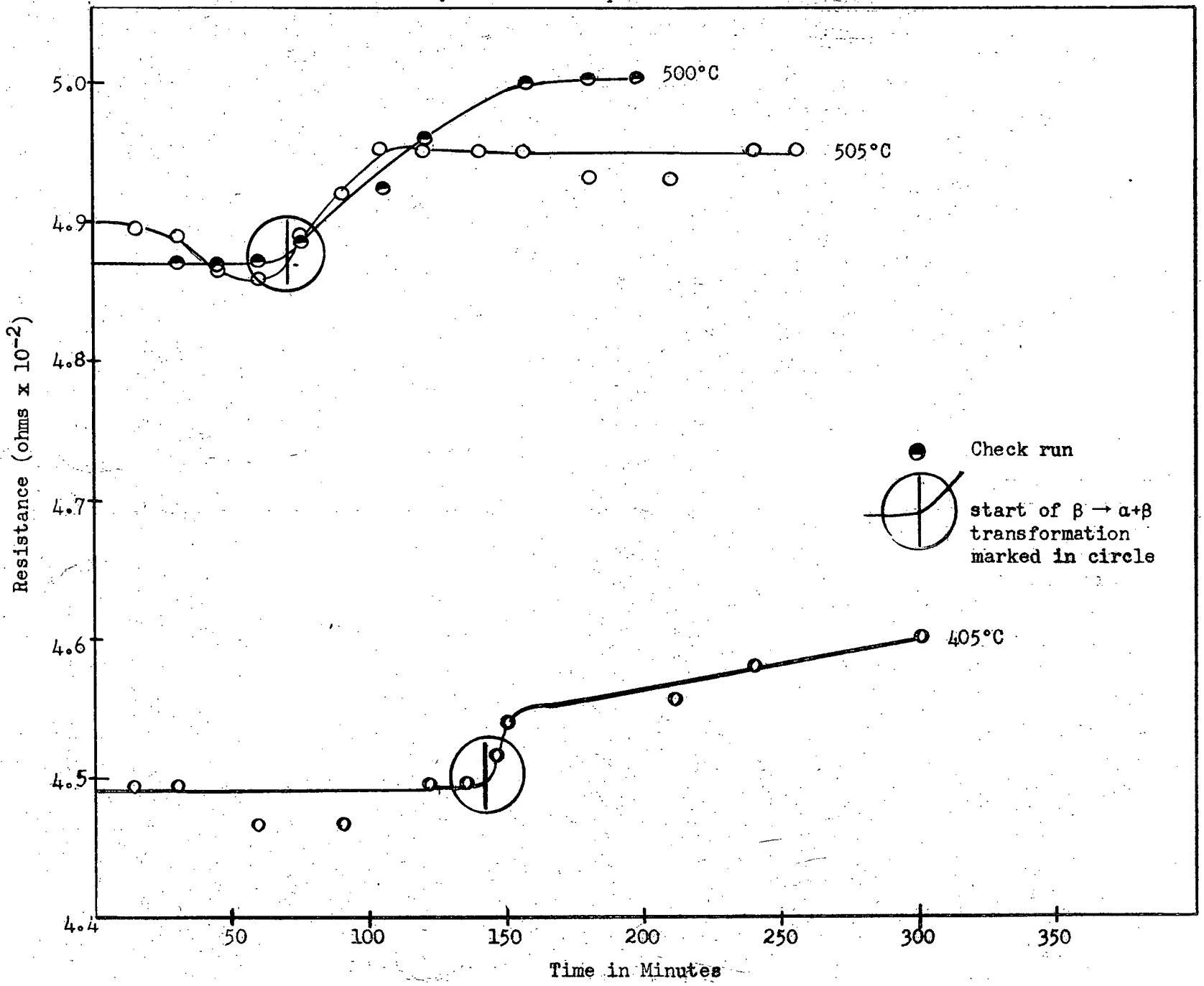

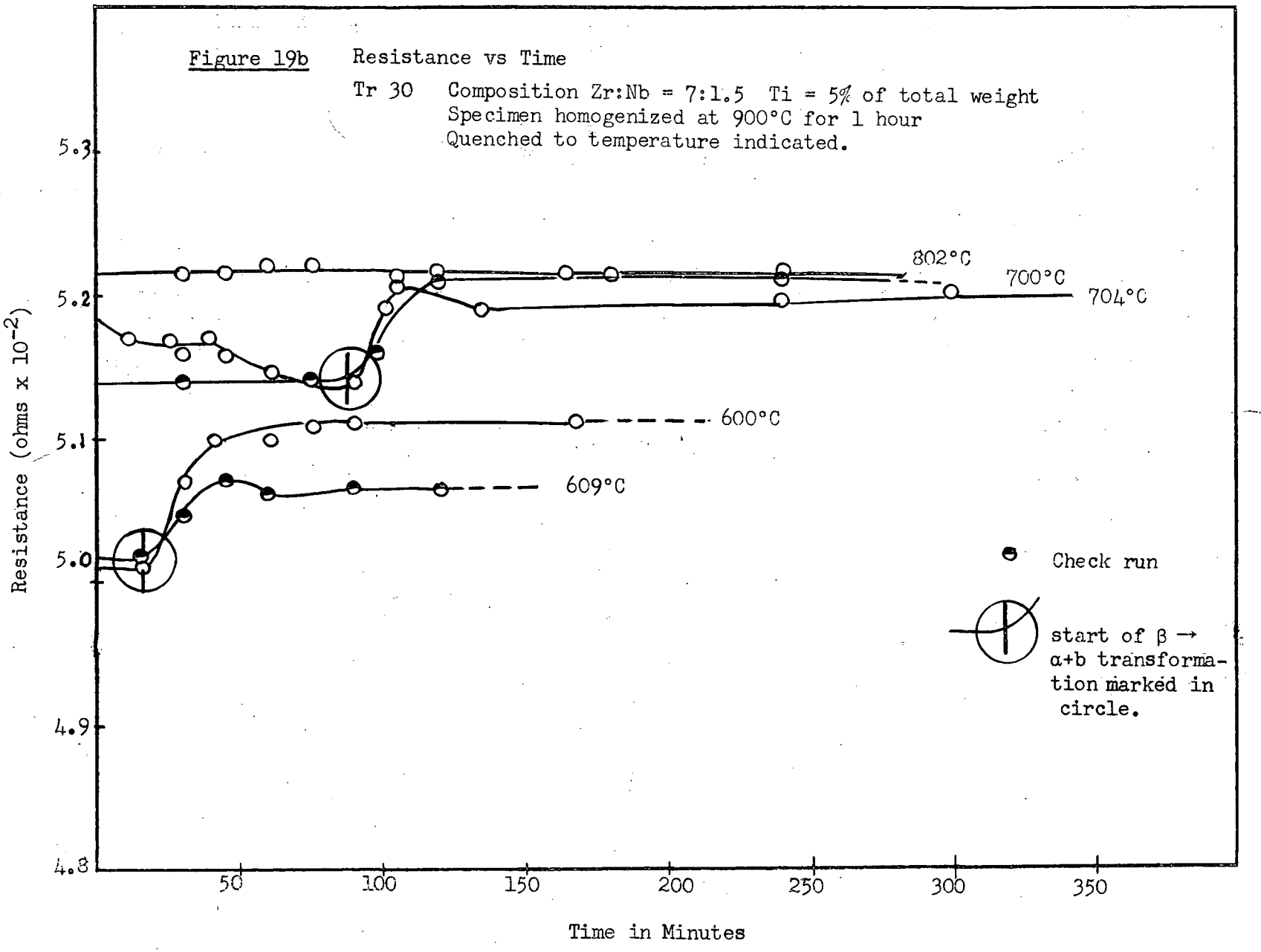
Figure 19b Resistance vs Time
Tr 30 Composition Zr:Nb = 7:1.5 Ti = 5% of total weight
Specimen homogenized at 900°C for 1 hour
Quenched to temperature indicated.
Resistance (ohms x 10^{-2})
5.3
5.2
5.1
5.0
4.9
4.8
50
100
150
200
250
300
350
Time in Minutes
802°C
700°C
704°C
600°C
609°C
Check run
start of β → α+b transformation marked in circle.

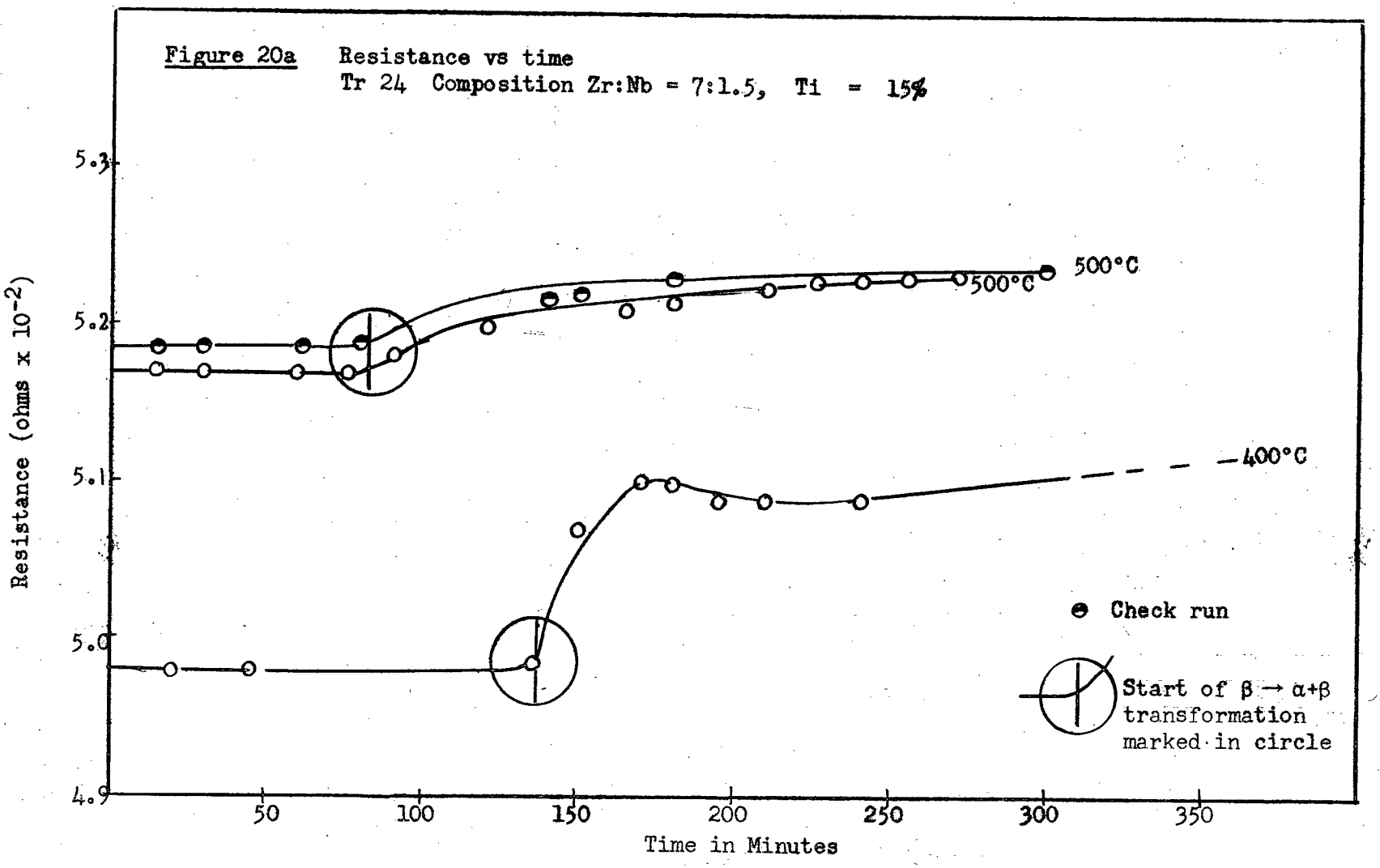
Figure 20a Resistance vs time
Tr 24 Composition Zr:Nb = 7:1.5, Ti = 15%
Resistance (ohms x 10^{-2})
5.3
5.2
5.1
5.0
4.9
50
100
150
200
250
300
350
Time in Minutes
500°C
500°C
400°C
Check run
Start of β → α+β transformation marked in circle

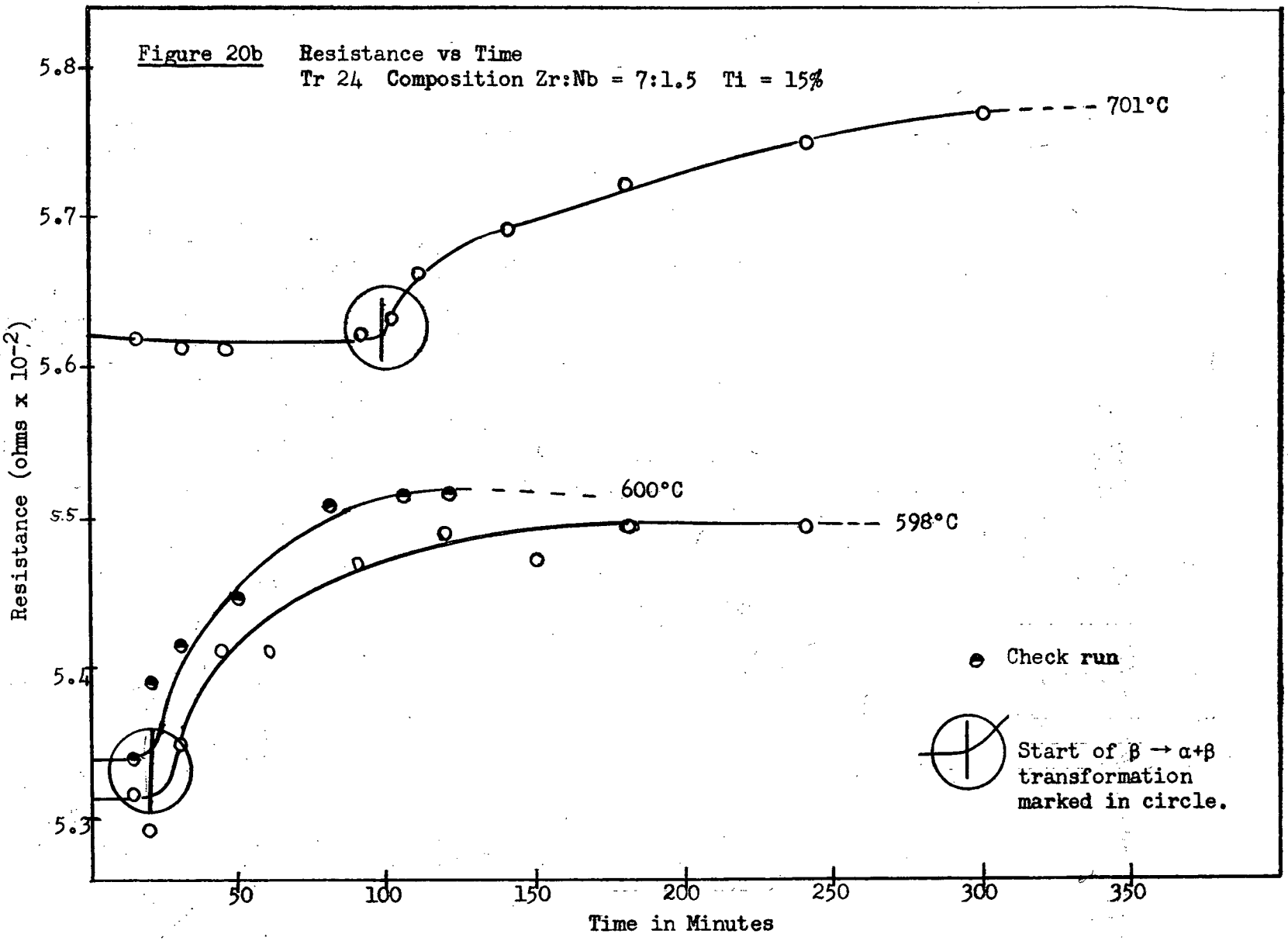
Figure 20b Resistance vs Time
Tr 24 Composition Zr:Nb = 7:1.5 Ti = 15%
701°C
600°C
598°C
Check run
Start of β → α+β transformation marked in circle.
Resistance (ohms x 10⁻²)
5.8
5.7
5.6
5.5
5.4
5.3
50
100
150
200
250
300
350
Time in Minutes

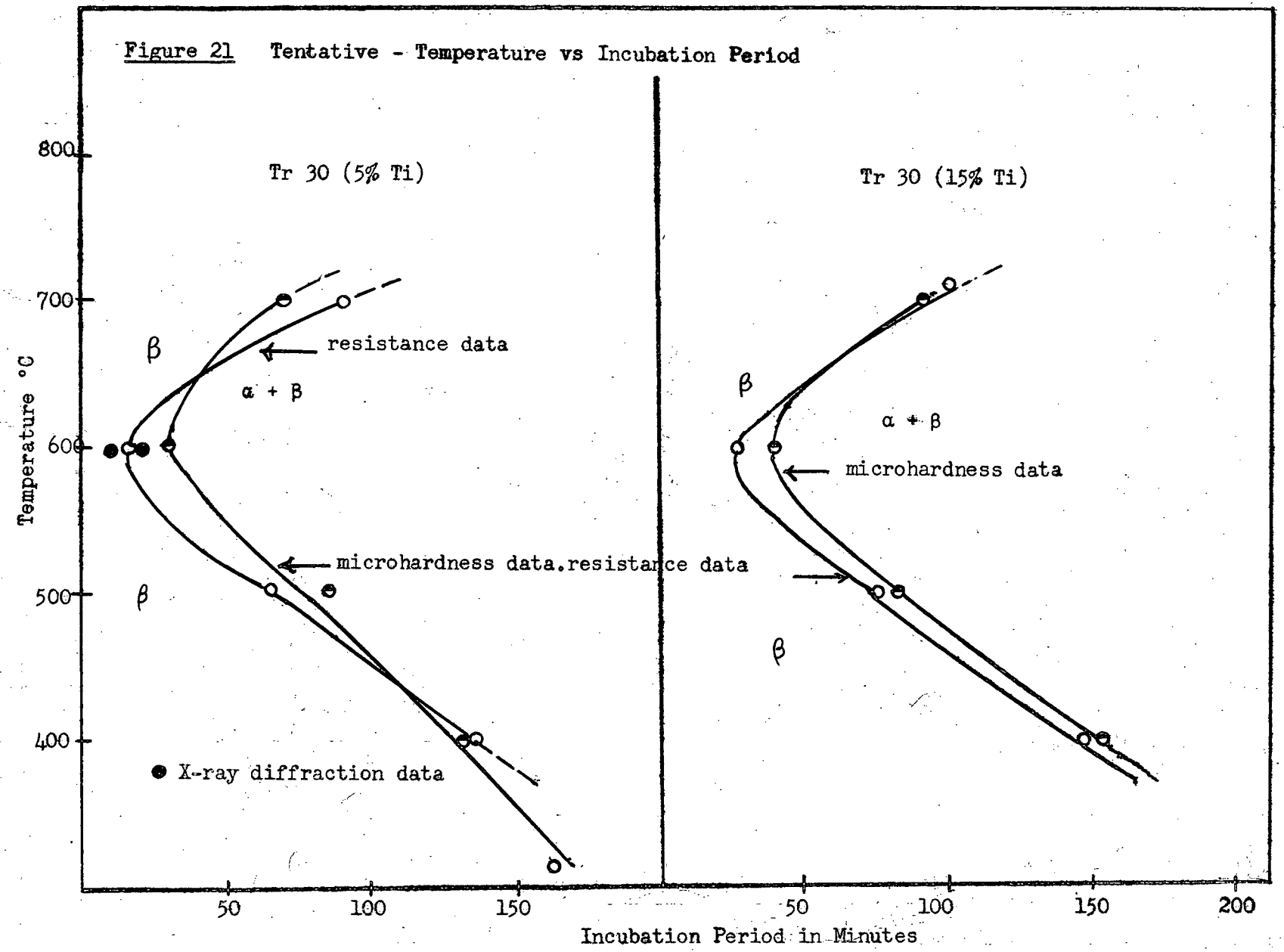
Figure 21 Tentative - Temperature vs Incubation Period
Tr 30 (5% Ti)
Tr 30 (15% Ti)
800
700
600
500
400
Temperature °C
β
α + β
resistance data
microhardness data.resistance data
β
X-ray diffraction data
β
α + β
microhardness data
β
50
100
150
50
100
150
200
Incubation Period in Minutes

into the close-packed hexagonal phase. This incubation period is smallest for a temperature of 600°C.

Given the resistivities of the individual components, it is impossible to predict the resistivity of a subsequent alloy. However, the resistance values reported correspond to resistivities that are not unreasonable. For the resistivity values of Finlayson[1] (Zr-16% Nb alloy), Domagala[6] (Zr-7% Nb, Z-=15% Nb alloys) and Domagala, Levinson and McPherson[7] (Zr-Mo alloys) are of the same order. These values lie between 60 and 120 micro-ohm-cm. Another trend that cannot easily be predicted is the phase that possesses the larger resistivity. The values of Finlayson show that above 500°C, the hexagonal alpha phase has higher resistivity than the body-centered cubic phase; while below this temperature, the reverse is true. The reports of Domagala[6] and Domagala[7] and co-workers show that the resistivity of the body-centered cubic phase is highest. Except for the fairly constant resistivity (resistance as plotted in Figure 19) at 800°C, the resistivity of the body-centered cubic phase in this investigation was lower than that of the hexagonal. This tendency is in agreement with the fact that extrapolation below 600°C leads to a lower body-centered phase resistance for a slowly heated wire specimen (Figure 18). As would be expected, resistances of the 15% titanium alloy (Tr 24) are higher than those of the alloy containing only 5%.

The curves generally show three main sections:

a) a flat portion representing the resistance of super-cooled beta phase, the duration of which marks the extent of the incubation period;
b) a rising portion representing the progress of transformation, $\alpha \rightarrow \alpha+\beta$;
c) another flat portion, the value of which is higher than (a). The resistance value is that of the alpha phase.

Now if the beta phase undergoes no transformation until the end of the incubation period, then the resistance of section (a) should be fairly constant. But the 500°C run (Figure 19) for example, shows a small variation although the period of incubation is reproduced by the check run. It is suggested that the variation was caused by temperature fluctuations. The variation (0.02 micro-ohm) corresponds to about 0.406 micro-ohm-cm. In order to cause such variation in resistance, the specimen temperature would only have to fluctuate 5°C (see linear relations of resistance and temperature in Figures 22 and 23). The specimen was attached to the ends of flexible thermocouple wires, the positioning of which depended only on their stiffness. Thus the specimen was not necessarily in the same position with the furnace from one run to the next. Furthermore, recorded specimen temperature is only from one small region. In view of these positioning difficulties, this region could be near the furnace windings in one run and not so near during the next run. Since temperature control is over the furnace (see position of control thermocouple in Figure 17) and not so much over the specimen, a difference of ten degrees could easily exist between the furnace temperature and the specimen temperature.

Finally, the sensitivity of detection and measurement of resistance is of interest. If the criterion for choice of method of measurement is the property of capacity, then it is assumed that the system -- i.e., the equipment and measuring device -- is amenable to early detection of change. It is shown in the analysis in Appendix CI that a transformation as small as one percent can be detected as a measurable change in resistance.

3. Micro-hardness Measurements.

Procedure

Sections less than an eighth of an inch thick were sawn from ingots Tr 29 and Tr 25; these alloys contained 5 and 15 percent titanium. Each slice

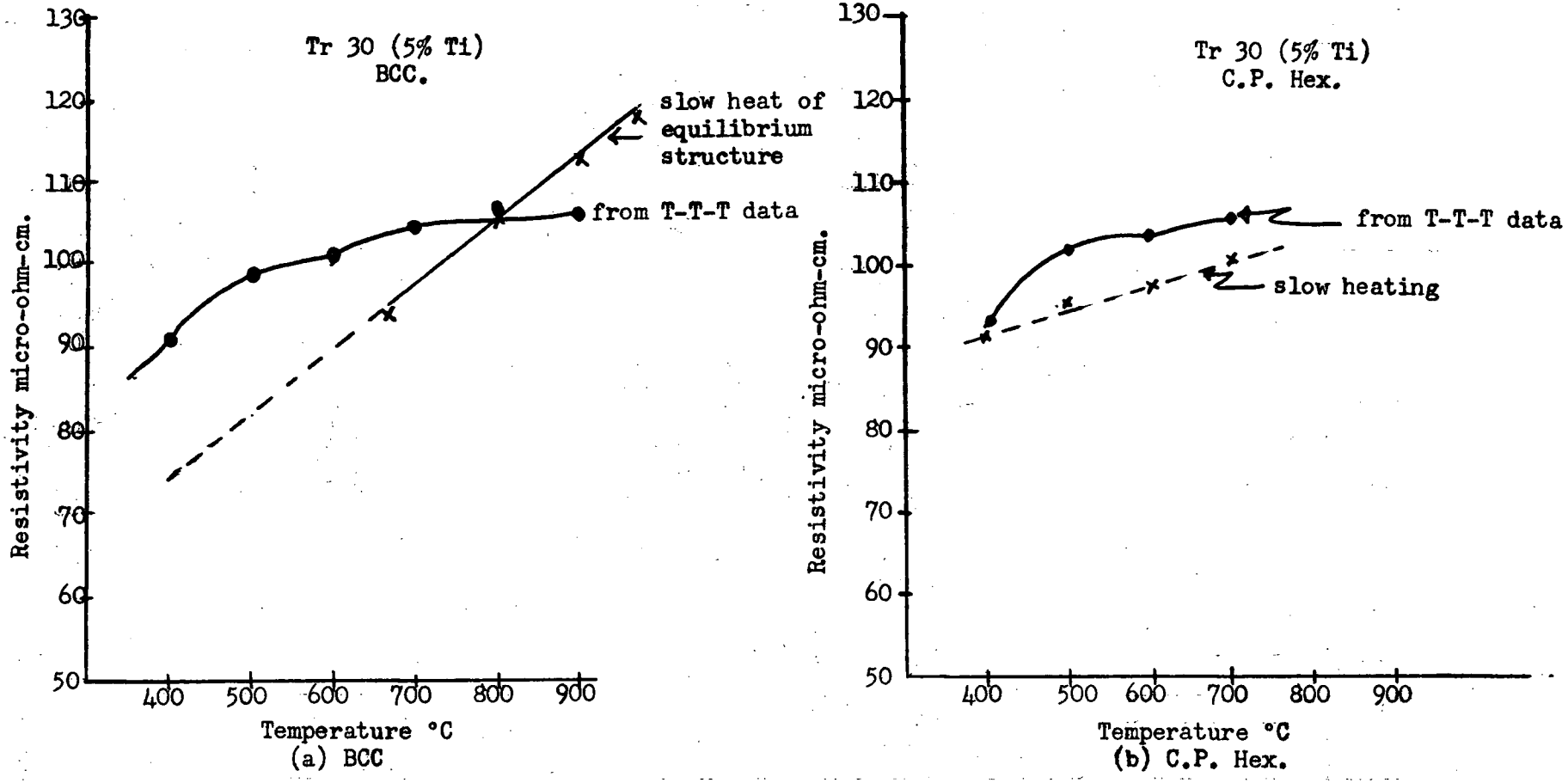

Figure 22. Resistivities of the two structures as found by slow heating and from isothermal transformation data.

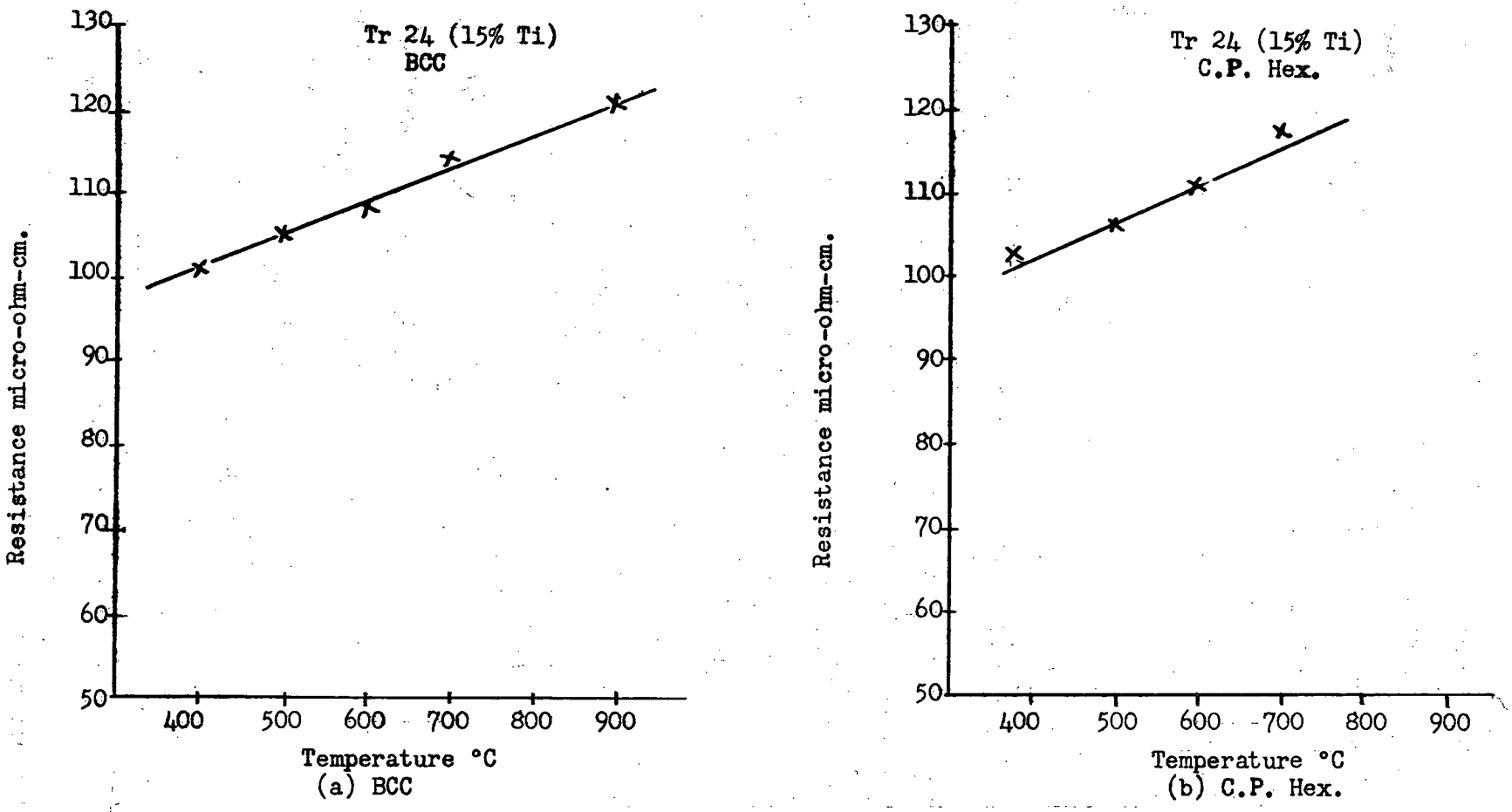

Figure 23. Resistivities of the two structures (isothermal transformation data)

was carefully wrapped in molybdenum foil and introduced into a vycor tube containing zirconium chips. The tube was then evacuated for twenty minutes and sealed. The specimens were then heat-treated according to the following schedule: all were homogenized at 900°C for an hour. Seven capsules were quickly transferred into a furnace maintained at 700 ± 5°C. The capsules were then quenched in cold water after 15 minutes, half an hour, one hour, two hours, four, eight and sixteen hours. Care was taken not break the capsule during quenching. A second batch of seven received similar treatment at 600°C. The procedure was repeated for 500°C. 400°C and 300°C. The specimens were mounted in lucite, polished and chemically etched with hydrofluoric acid containing a little lactic acid and a few drops of nitric acid.

Micro-hardness measurements were taken on each specimen with a Bergsman microhardness tester mounted on a Leitz Metallograph. The load employed was 100 gm. and duration of impingement was fifteen seconds. Ten impressions were made on each specimen. The arithmetic mean and standard deviation of their Diamond Pyramid Hardness are plotted in Figures 24 and 25. On these curves the approximate position indicating the start of the $\beta \rightarrow \alpha+\beta$ reaction is marked.

Results and discussion

From the above description of procedure it can be seen that at best the reactions in the wire specimens (resistance measurements) are only crudely reproduced in the heat-treated pieces. Dissimilar size and shape of specimens, poor vacuum in the heat treatment, and quenching difficulties could very easily affect the reactions. However, even more important are the differences of opinion on the methods for micro-hardness testing. Wilson[27] suggests that in order to make quantitative measurements of the mechanical properties of the surface layer, much precaution is necessary. It is necessary to have an

Figure 24a. Microhardness Plots - Tr 29 (5% Ti)

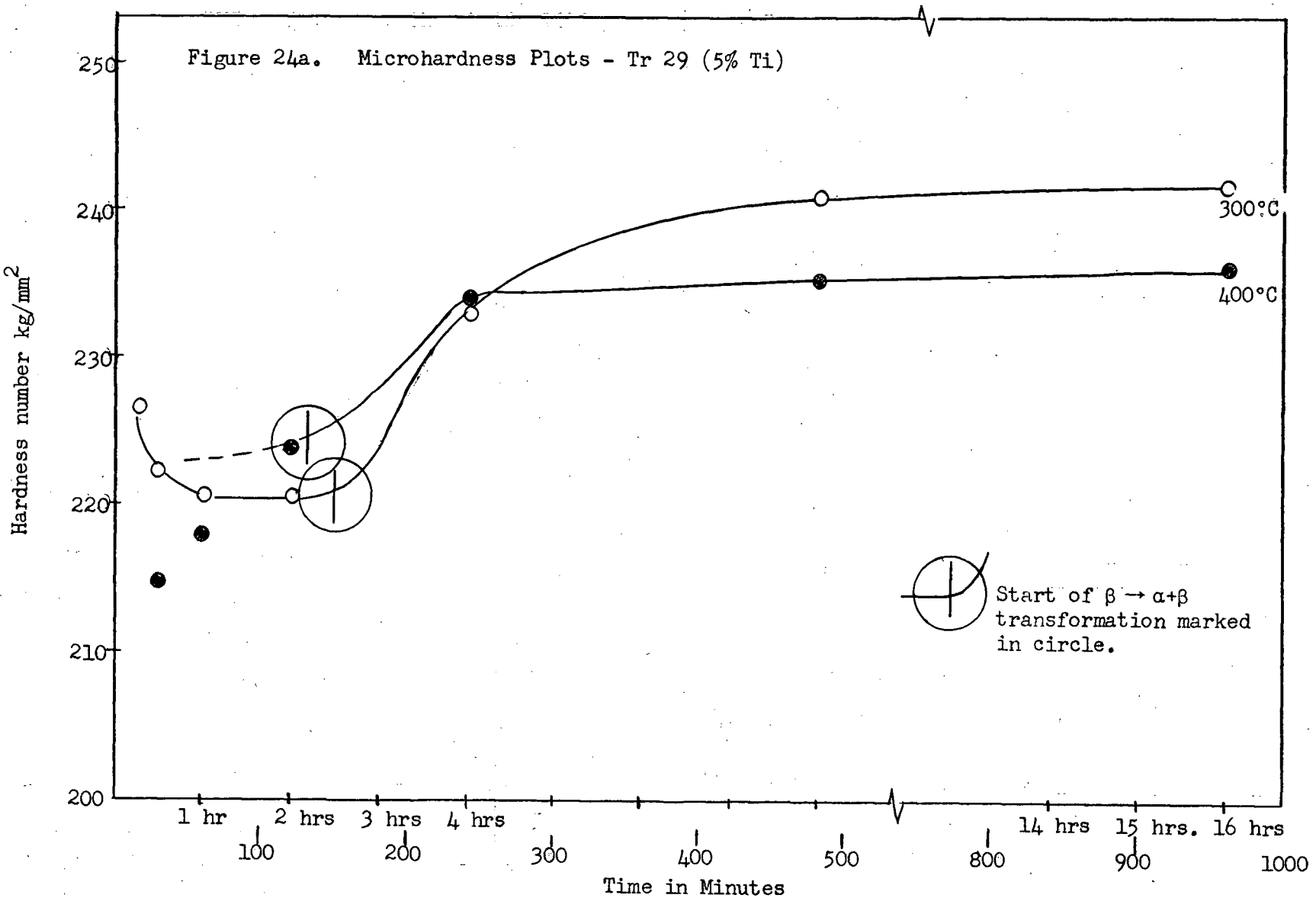

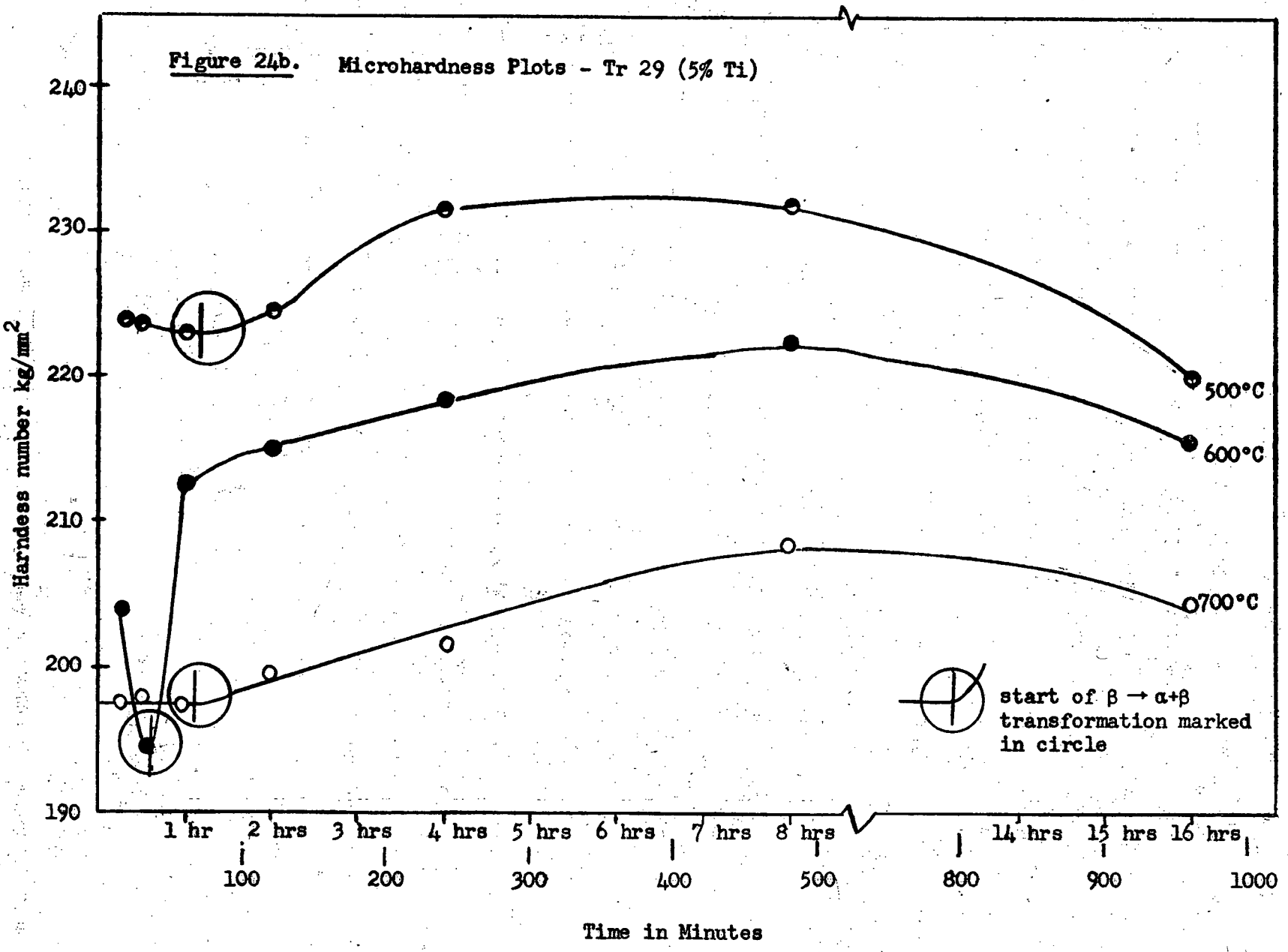
Figure 24b. Microhardness Plots - Tr 29 (5% Ti)
240
230
220
210
200
190
Harndess number kg/mm2
500°C
600°C
700°C
start of β → α+β transformation marked in circle
1 hr
2 hrs
3 hrs
4 hrs
5 hrs
6 hrs
7 hrs
8 hrs
14 hrs
15 hrs
16 hrs
100
200
300
400
500
800
900
1000
Time in Minutes

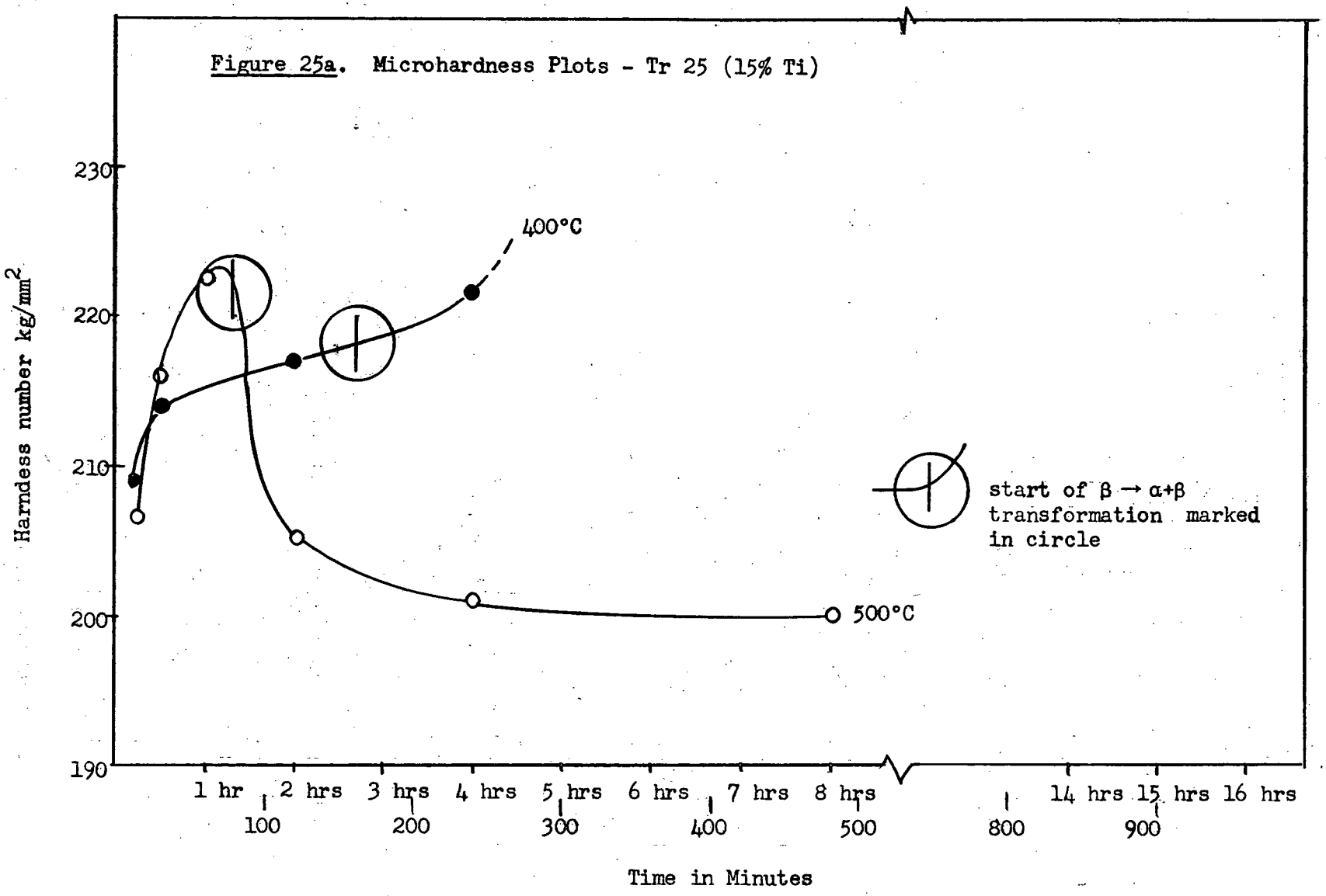
Figure 25a. Microhardness Plots - Tr 25 (15% Ti)
Harndess number kg/mm2
230
220
210
200
190
400°C
500°C
start of β → α+β transformation marked in circle
1 hr
2 hrs
3 hrs
4 hrs
5 hrs
6 hrs
7 hrs
8 hrs
14 hrs
15 hrs
16 hrs
100
200
300
400
500
800
900
Time in Minutes

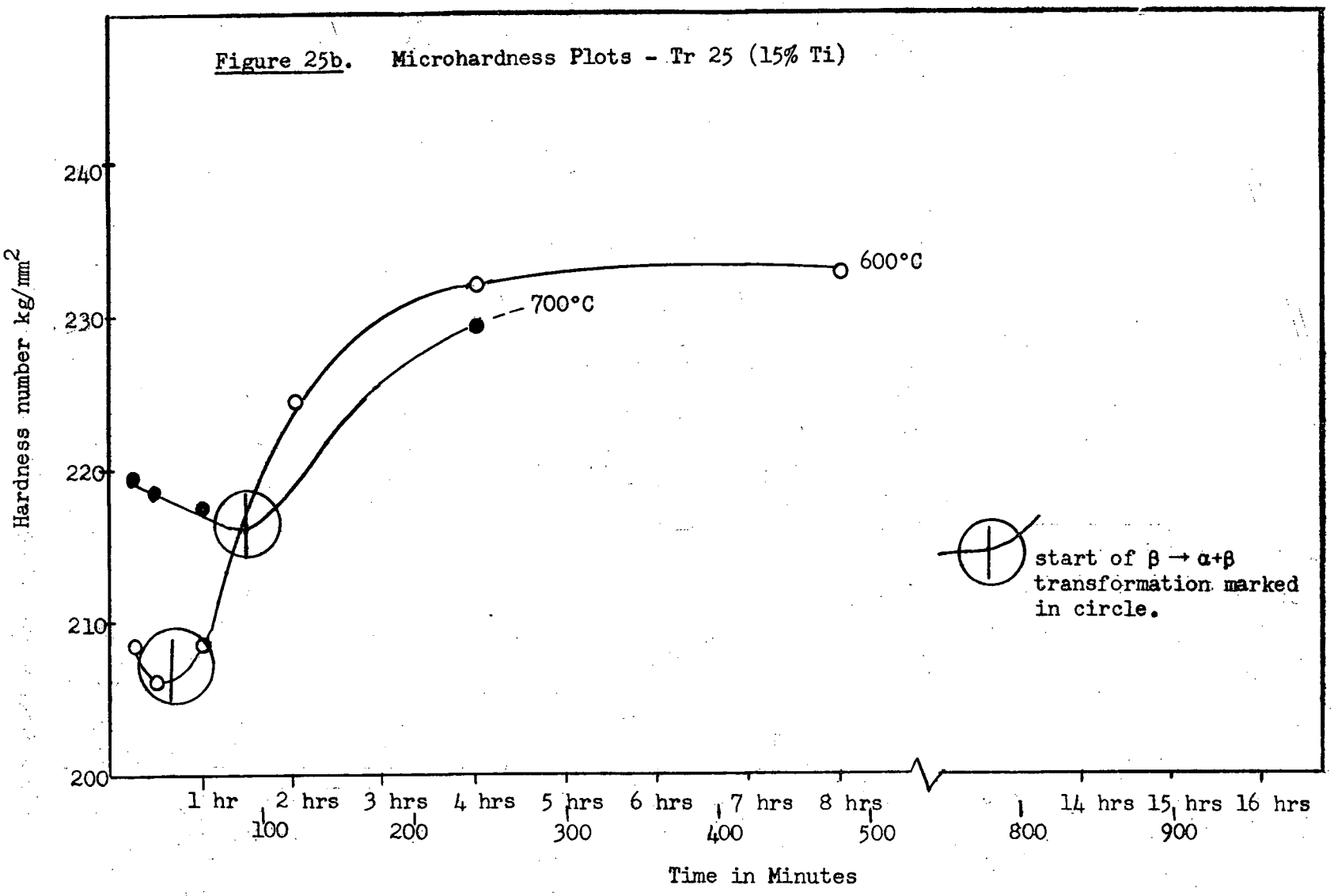
Figure 25b. Microhardness Plots - Tr 25 (15% Ti)
Hardness number kg/mm2
240
230
220
210
200
600°C
700°C
start of β → α+β transformation marked in circle.
1 hr
2 hrs
3 hrs
4 hrs
5 hrs
6 hrs
7 hrs
8 hrs
14 hrs
15 hrs
16 hrs
100
200
300
400
500
800
900
Time in Minutes

absolutely pure specimen, to anneal perfectly, to electropolish, to handle it with extreme care before testing, and to use a diamond point that has a real point. It is also necessary to eliminate as far as practicable, all sources of vibration, and this includes switching off the illuminating system while the indentation is being made. The effects of grain boundaries and orientation cannot be neglected, for hardness values can show a considerable scatter (as indicated by the large deviations in the data) if spread over an area. In view of all this, interpretation of the reported measurements should be made with reservation. In some of the curves, it is not too difficult to point out fairly constant initial hardness corresponding to the incubation period. However, the general effect of addition of titanium is not easily discerned. The hardness data is included in Appendix E.

4. Metallographic

Results and discussions

Figures 25, 27, 28, 29, 30 and 31 show the results of metallographic examination. Figure 26 shows the familiar needles of a hydride phase in an alloy containing 5% titanium. It reveals the persistent nature of these needles, for the specimen has been held at 400°C for half an hour. According to the resistance data, no transformation has occurred during this time. The other photomicrographs show that the retained beta phase etches white. The formation of a second phase including the hydride needles can be observed as superimposed dark areas or particles. Figures 29 and 30 compare the structures of a specimen (5% Ti) kept at 600°C for a week and a transformed wire specimen. Difficulty of etching increases with progressive transformation as can be observed in Figure 29. Etching difficulties coupled with the presence of the hydride phase make the analysis of these photomicrographs difficult.

Figure 26. (5% Ti) alloy held at 400°C for 30 min. Persisting hydride needles and untransformed beta - X300. Etch HF+HNO_3+lactic acid.

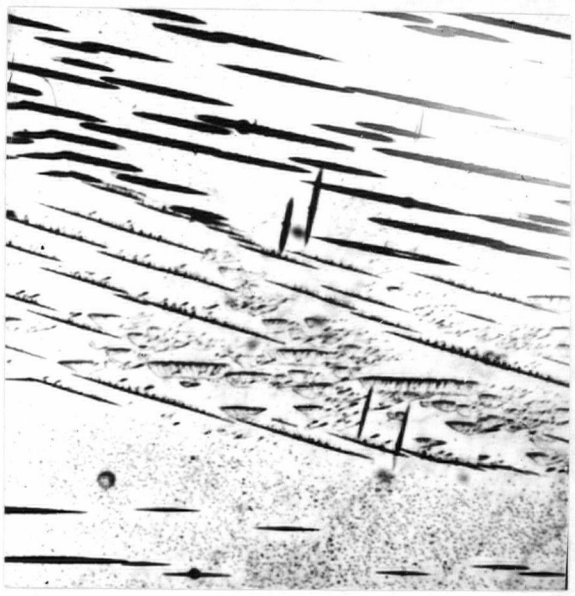

Figure 27. (5% Ti) alloy held at 500°C for 30 min. Mostly beta + needles X300. Etch HF+HNO_3+lactic acid.

Figure 28. (5% Ti) alloy held at 500°C for 4 hrs. Transformed beta, needles still in evidence X300.

Figure 29. (5% Ti) alloy held at 500°C for 8 hrs. X800.

Figure 30. (5% Ti) alloy held at 600°C for 1 week. Transformed beta X300.

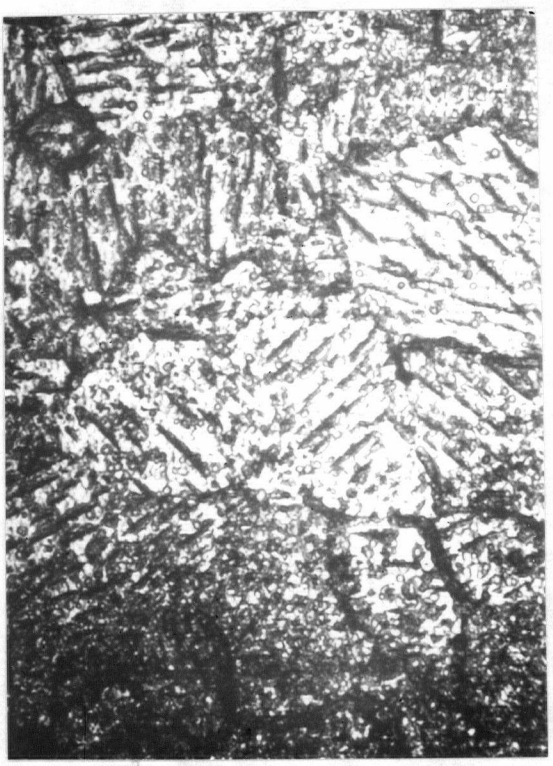

Figure 31. Wire specimen transformed at 600°C for 5 hours X300.

5. X-ray Diffraction

Procedure

Preparation of powder samples from alloys presented difficulties. Diffuse lines indicated that the powder was only partially annealed even though the annealing temperature was increased to 450°C. Complete anneal was at the expense of further transformation. This problem was partly solved by inserting the wire specimens in the camera and taking diffraction pictures of these. The specimens were carefully etched to pin size in a solution of hydrofluoric acid and lactic acid. Filtered K α copper radiation was used. The best results were obtained by placing the nickel filter inside the camera, cutting the power down to 25 KV and exposing for a period of at least two hours at 15 ma.

Results and discussion

The data shown in Appendix F are for the 5% titanium alloy held at 600°C for only ten minutes and a supposedly transformed specimen at the same temperature. The specimen held at 600°C for ten minutes showed only body-centered lines. Unless impurity lines were so weak as to cause them to be hardly discernible, it should be assumed that the alloys did not contain large amounts of impurity.

The d-spacings were slightly smaller than those determined by Whitmore: the wire specimens, however, were not necessarily in the equilibrium condition; furthermore, Whitmore employed powder specimens and not wire specimens. The transformed specimen showed hexagonal lines as well as body-centered lines. These body-centered lines could be a mixture of beta lines of the solution and beta lines of niobium or all beta lines of niobium. Because the d-spacings are generally low, indexing by comparison with the

National Bureau of Standards values would be difficult. However, if the specimen were fully transformed, then the body-centered lines must all be reflections from beta niobium.

A specimen held at 600°C for 20 minutes showed the usual body-centered lines and weak hexagonal lines at the low angle side. Another specimen transformed at 500°C for 8 hours, showed hexagonal lines and body-centered lines. A supposedly transformed 15% titanium alloy showed strong body-centered lines and weak hexagonal ones. The hexagonal lines at the high angle side were quite diffuse. All these specimens did not give sharp lines suitable for measurement; the resulting pictures were therefore only studied and compared.

If comprehensive X-ray data were desired then the method to be employed, i.e., powder or wire at room temperature, must be anticipated and planned. This suggestion has only been evident from the difficulties encountered. For instance, small pieces that were salvaged from the experiment were filed in order to obtain powder specimens; the latter were discarded in favour of wire specimens. Again, if a transformed wire specimen were kept at temperature for longer periods, then grain growth would reduce the number of crystals and cause numerous spots without any apparent order on the film.

III. CONCLUSIONS

The results of this investigation have shown that the effect of small additions of titanium on the incubation period which precedes the $\beta \rightarrow \alpha+\beta$ reaction in an isothermally transformed zirconium-17.6% niobium alloy is to prolong it. This effect has been demonstrated by establishing and comparing the relation between the incubation period and temperature for two alloys; the first containing 5% titanium and the second, 15% titanium. The investigation has been accomplished primarily by means of electrical resistance measurements in conjunction with micro-hardness tests, metallographic examination and X-ray diffraction methods.

According to electrical resistance data, an alloy containing 5% titanium shows incubation periods of approximately 80, 15, 65 and 135 minutes at corresponding temperatures of 700°C, 600°C, 500°C and 400°C. The minimum in the time is in the vicinity of 600°C. In order to establish its exact position more data is necessary. The addition of 15% titanium to the zirconium-17.6% niobium alloy caused the incubation period to be extended. At 600°C, this period is approximately 25 minutes as compared to the 15 minutes observed in a 5% titanium alloy. Here too, the precise position of the minimum in the time is unknown. It is reasonable to suppose that it exists at some temperature slightly below that of the alloy containing 5% titanium. The increase in the incubation period shown by the addition of 15% titanium is not uniform. For above and below 600°C, the interval decreases progressively so that at some temperature above 700°C and below 400°C, it approaches zero.

The electrical resistance data does not indicate the presence of intermediate products during the ensuing isothermal transformation. However,

it is believed that more data is necessary to establish this fact.

Micro-hardness tests reveal that although the primary effect of small additions of titanium is to prolong the incubation period, the period of incubation is longer than the value obtained from electrical resistance. For, at 600°C, the alloy containing 5% titanium shows an incubation period of approximately 30 minutes as compared to the 15 minutes obtained from resistance data. The micro-hardness tests show that when the amount of titanium is increased to 15%, the incubation period becomes 40 minutes. The observation of a longer incubation period in the micro-hardness specimens is not unreasonable since the shape, size and heat-treatment of these did not exactly duplicate those of the resistance specimens.

Metallographic and X-ray diffraction data are limited. Although they do not clearly establish the limits of incubation periods at the various temperatures, the data do not conflict with those obtained by electrical resistance and micro-hardness measurements.

That alloy additions should generally lengthen the incubation period is in keeping with modern views on alloying theory and practice. Recent studies of Domagala[6] on zirconium-niobium alloys and of Domagala and coworkers[7] on zirconium-molybdenum alloys have been cited as showing this general effect.

Furthermore, the desirability of observing isothermal transformation with resistance measurements has been clearly demonstrated. In view of its high sensitivity and ease of measurement, electrical resistance determinations could form the basis of further experimental work on this system. Micro-hardness, metallographic and X-ray diffraction methods would prove invaluable in these studies.

APPENDIX A

Related Phase Diagrams

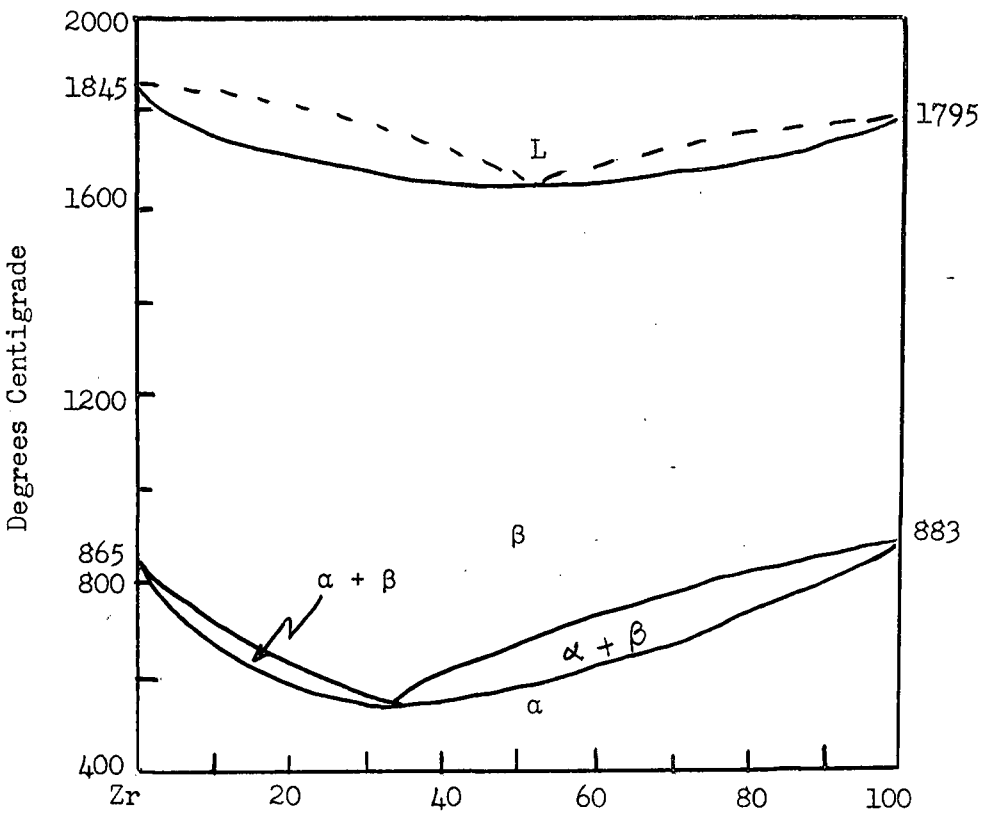

1. The zirconium-titanium constitutional diagram (after Fast and Hayes et al)

APPENDIX A (cont'd.)

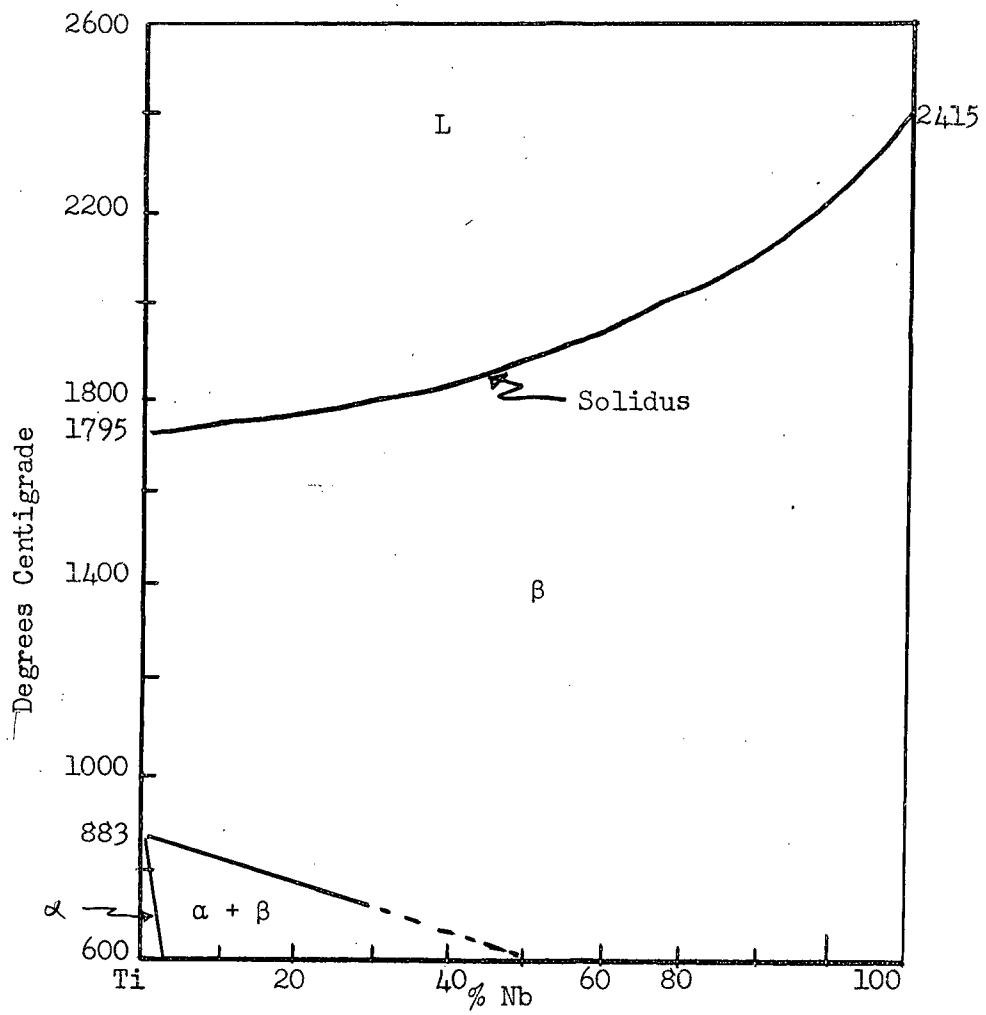

2. The titanium-niobium constitutional diagram (after Hansen et al)

APPENDIX B

Related Phase Diagrams (Impurities)

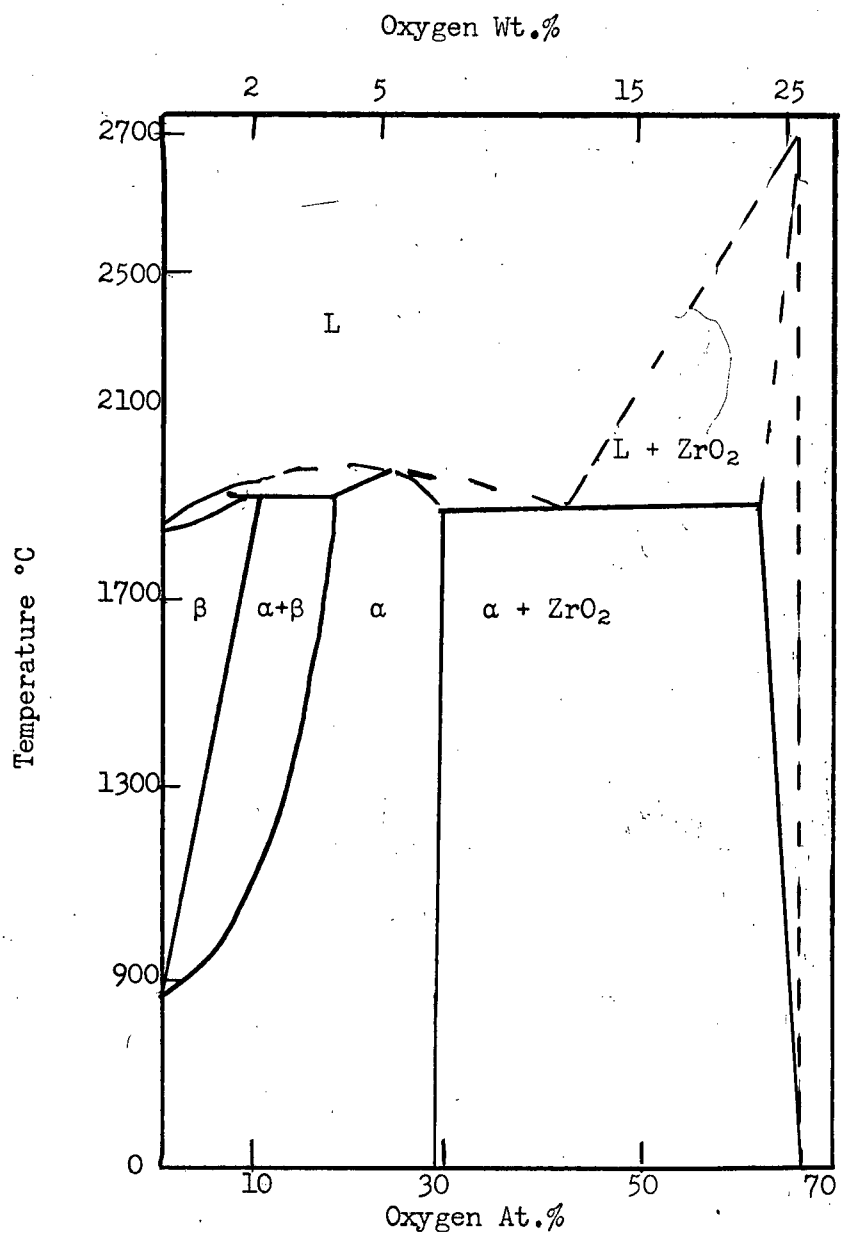

1. The zirconium-oxygen system

APPENDIX B (cont'd.)

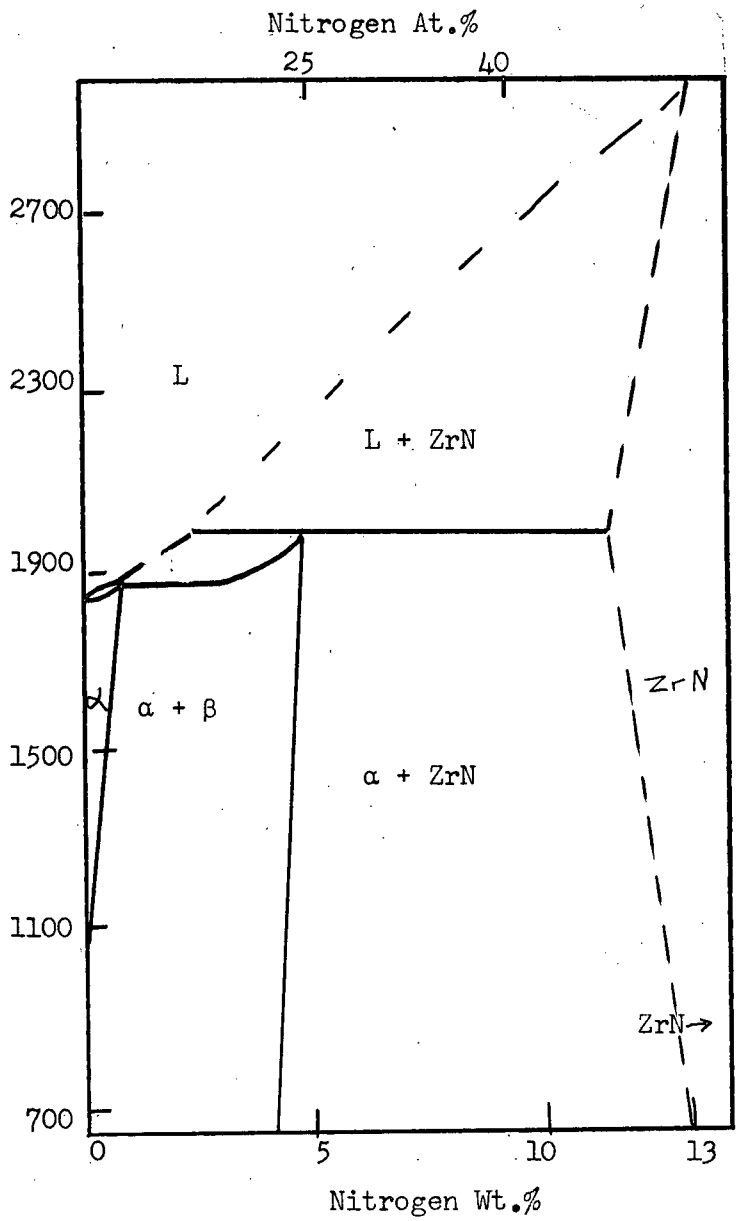

2. The zirconium-nitrogen system

APPENDIX B (cont'd.)

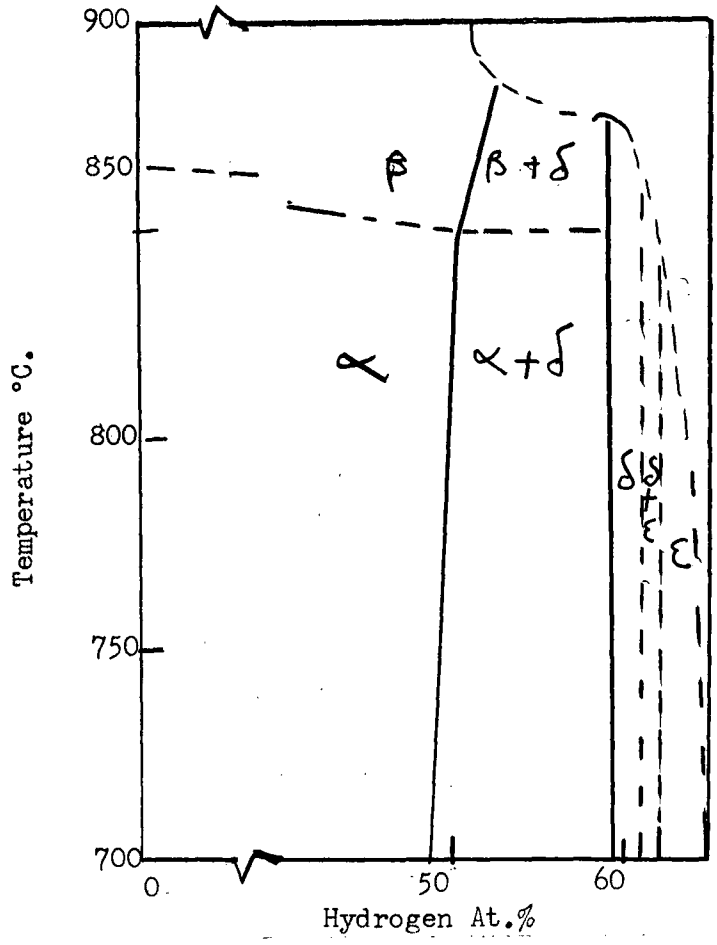

3. The zirconium-hydrogen system

APPENDIX CI

To show that electrical resistance as employed in this investigation is a 'capacity property'.

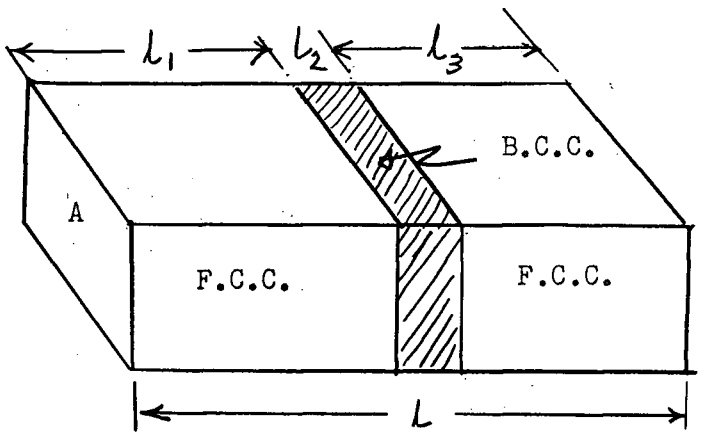

Figure 1. A transformation block showing F.C.C. changing into B.C.C. (Resistance in Series).

If the resistance $R = \frac{\ell}{A}$ where ℓ is length of block
A area marked in Figure 1
σ specific conductance

then $R = S\frac{l}{A}$ where S is $\frac{1}{\sigma}$

(No transformation) $R_1 = \frac{S_{FCC}\,\ell}{A} = \frac{\ell}{\sigma_{FCC}A}$

(Some transformation) $R_2 = R_{FCC} + R_{BCC} + R_{FCC}$

$$= \frac{S_{FCC}\,\ell_1}{A} + \frac{S_{BCC}\,\ell_2}{A} + \frac{S_{FCC}\,\ell_3}{A}$$

$$= \frac{\ell_1 + \ell_3}{\sigma_{FCC}A} + \frac{\ell_2}{\sigma_{BCC}A}$$

If $\sigma_{FCC} \neq \sigma_{BCC}$

Then $R_1 \neq R_2$ ⟵

Appendix CI (cont'd.)

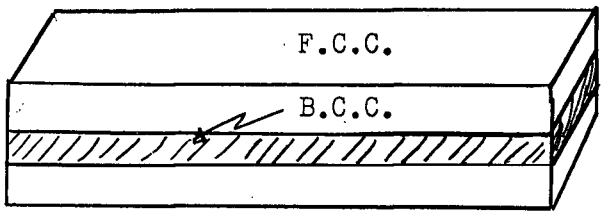

Figure 2. Transforming block (resistance in parallel)

The condition in Figure 2 is equivalent to resistances R_1 and R_2 in parallel

$$R_1 = \frac{R_1 R_2}{R_1+R_2}$$

$$\frac{dR}{dR_1} = \frac{R_2 (R_1+R_2) - R_1R_2}{(R_1+R_2)^2}$$

$$= \frac{R^2}{(R_1+R_2)^2}$$ this is a perfect square

therefore > 0

The above analyses show that a change in the amount of some phase in the block will register a change in resistance for the whole block.

APPENDIX CII

In order to estimate the inherent error in the fixing of the incubation period, it would be necessary to know the degree of response in the potentiometer -- i.e. the amount of transformation that causes a detectable change in resistance. Such error is estimated in the ensuing analysis.

Resistances

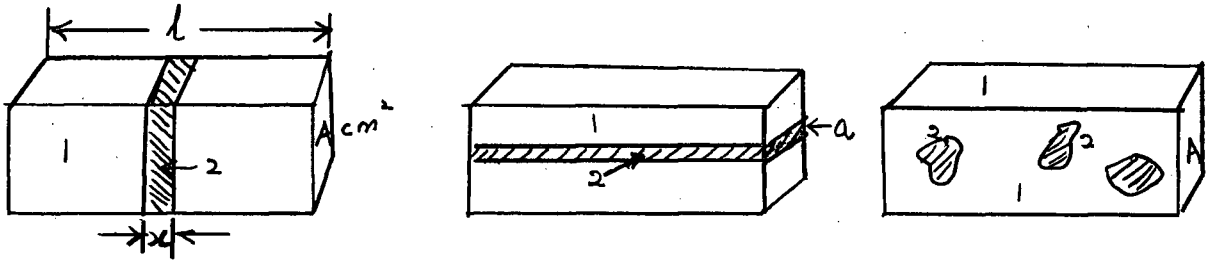

(a) Series (b) Parallel (c) Actual state of affairs in specimen

Let r_o ohms be the detectable change in resistance;

and resistivity of phase 1 (say bcc) be ρ_1 ohm cm,

and resistivity of phase 2 (c.p.hex) be ρ_2 ohm cm.

Suppose the shaded region x as shown above has transformed, the the resistance of the specimen = $R_1' + R_2'$ [series as in (a) above]

$$= \frac{(l - x)\rho_1}{A} + \frac{x\rho_2}{A} \qquad (1)$$

where A is the cross sectional area

and l the length of the wire specimen.

The change in resistance = (new resistance) - (initial resistance)

$$= \frac{(l - x)\rho_1}{A} + \frac{x\rho_2}{A} - \frac{l\rho_1}{A}$$

$$= \frac{-x\rho_1}{A} + \frac{x\rho_2}{A}$$

$$= \frac{x}{A}(\rho_2 - \rho_1) \qquad (2)$$

Appendix CII (Cont'd.)

Minimum x detectable by change in resistance is x_o

$$\text{where} \quad \frac{x_o}{A}(\rho_2 - \rho_1) = r_o \qquad (3)$$

If α is the fraction transformed,

$$\text{then} \quad \alpha = \frac{xA}{\ell A} = \frac{x}{\ell} \qquad (4)$$

Therefore minimum α detectable by resistance measurement is α_o

$$\text{where } \alpha_o = \frac{x_o}{\ell}$$

$$\text{which by substitution from (3)} = \frac{1}{\ell}\left[\frac{r_o A}{\rho_2 - \rho_1}\right] \qquad (5)$$

$$\text{now} \quad \frac{\rho_2 \ell}{A} = R_2$$

$$\text{and} \quad \frac{\rho_1 \ell}{A} = R_1$$

where R_2 is the total resistance after transformation is complete, i.e. $x = \ell$, and R_1 is the initial resistance before transformation starts, i.e. $x = 0$.

Employing the above expressions for R_1 and R_2, (5) becomes

$$\alpha_o = \frac{r_o}{R_2 - R_1}$$

$$= \frac{ir_o}{iR_o - iR_1} \qquad \text{where i is current}$$

$$= \frac{V_o}{V_2 - V_1} \qquad \text{where V is potentiometer reading.}$$

Now suppose a change of 0.001 millivolts can be read on the potentiometer, then at say 600°C (Figure 19),

$$\alpha_o = \frac{0.001}{5.12 - 5.01}$$

$$= \frac{0.001}{0.11} \approx 0.01$$

Appendix CII (Cont'd.)

Therefore a resistance measurement detects a transformation of 1% in the wire specimen.

If the transformation is as shown in (b), then the resistances are parallel. If the small transformed section has area a, then the resistance R_1 of the specimen is:

$$R = \left(\frac{1}{R_1'} + \frac{1}{R_2'}\right)^{-1} \qquad (6)$$

where $R_1' = \frac{\rho_1 \ell}{(A - a)}$

thus $R = \left[\frac{(A - a)}{\rho_1 \ell} + \frac{a}{\rho_2 \ell}\right]^{-1}$

initial resistance $= \frac{\rho_1 \ell}{A}$

Therefore change in resistance $= \left[\frac{(A - a)}{\rho_1 \ell} + \frac{a}{\rho_2 \ell}\right]^{-1} - \frac{\rho_1 \ell}{A}$ (7)

Let α be the fraction transformed,

then $\alpha = \frac{\ell a}{\ell A} = \frac{a}{A}$

thus α detectable is α_o

where $\alpha_o = \frac{a_o}{A}$ (8)

If the minimum a detectable is a_o,

then from (7), $\left[\frac{(A - a)}{\rho_1 \ell} + \frac{a_o}{\rho_2 \ell}\right]^{-1} \frac{\rho_1 \ell}{A} = r_o$ (9)

where r_o is the minimum detectable change in resistance.

Appendix CII (cont'd.)

To find a in terms of r , Equation (9) becomes,

$$l\left(\frac{A - a_o}{\rho_1} + \frac{a_o}{\rho_2}\right)^{-1} - \rho_1 \frac{l}{A} = r_o$$

$$\left[\frac{(A - a_o) + a_o\rho_1}{\rho_1 \rho_2}\right]^{-1} - \frac{\rho_1}{A} = \frac{r_o}{l}$$

$$\frac{\rho_1 \rho_2}{(A - a_o)\rho_2 + a_o\rho_1} - \frac{\rho_1}{A} = \frac{r_o}{l}$$

$$\frac{\rho_1 \rho_2}{(A - a_o)\rho_2 + a_o\rho_1} = \frac{\rho_1}{A} + \frac{r_o}{l}$$

or

$$\frac{(A - a_o)\rho_2 + a\rho_1}{\rho_1 \rho_2} = \left[\frac{r_o}{l} + \frac{\rho_1}{A}\right]^{-1}$$

$$A\rho_2 - a_o(\rho_2 - \rho_1) = \rho_1 \rho_2 \left(\frac{r_o A + \rho_1 l}{A}\right)^{-1}$$

$$A\rho_2 - \frac{\rho_1 \rho_2 l A}{r_o A + \rho_1 l} = a\,(\rho_2 - \rho_1)$$

$$a_o = \frac{1}{(\rho_2 - \rho_1)}\left[A\rho_2 - \frac{\rho_1 \rho_2 l A}{r_o A + \rho_1}\right.$$

therefore

$$\alpha_o = \frac{\rho_2 A}{A(\rho_2 - \rho_1)}\left[1 - \frac{\rho_1 l}{r_o A + \rho_1 l}\right]$$

$$= \frac{\rho_2}{(\rho_2 - \rho_1)}\left[\frac{r_o A + \cancel{\rho_1 l} - \cancel{\rho_1 l}}{r_o A + \rho_1 l}\right]$$

$$= \frac{\rho_2 \; r_o A}{(\rho_2 - \rho_1)\,(r\,A + \rho_1 l)} \qquad (10)$$

Appendix CII (cont'd.)

Now $\rho_1 = \frac{A}{\ell} R_1$ where R_1 is initial resistance, i.e., a = 0

$= \frac{A}{\ell} \frac{V_1}{i}$ where V is potential and i, current.

Similarly $\rho_2 = \frac{A}{\ell} \frac{V_2}{i}$

and $r_o = \frac{V_o}{i}$

Thus from Equation (10), $\alpha_o = \left(\frac{A}{\ell} \frac{V_2}{i}\right) \frac{V_o}{i} \frac{1}{\frac{A}{\ell i}(V_2 - V_1)} \frac{1}{\left(\frac{V_o A}{i} - \frac{A V_1}{i}\right)}$

$$= \frac{A \quad V_2 \; V_o \quad i}{i \; (V_2 - V_1) A (V_o + V_1)}$$

$$= \frac{V_2 V_o}{(V_2 - V_1)\,(V_o + V_1)}$$

Thus at 600°C (5% titanium alloy)

$V = 0.001$ mv.
$V_2 = 5.12$ mv.
$V_1 = 5.01$ mv.

and $\alpha_o = \frac{5.12(0.001)}{0.11(5.011)}$

≈ 0.01

Therefore resistance measurement detects a transformation of 1% of the specimen.

The actual process of transformation, however, will be more like that shown in (c), i.e., several nucleation sites. The probable value of α_o will therefore lie between that of 'series' treatment and that of the 'parallel' treatment. According to the above analysis, 1% is the detectable fractional volume of transformation.

APPENDIX D

Resistance Data

Resistance values are in ohms x 10^{-2}
Time is in hours.
Tr 30 - 5% titanium alloy
* indicates fresh specimen.

802°C *		704°C *		700°C		600°C *		609°C *		505°C *		500°C		405°C *	
t	R	t	R	t	R	t	R	t	R	t	R	t	R	t	R
0.0	5.215	0.0	5.18	0.0	5.14	0.0	5.01	0.0	5.015	0.0	4.9	0.0	4.87	0.0	4.495
0.083	5.215	0.083	5.18	0.5	5.14	0.083	5.01	0.083	5.015	0.25	4.895	0.5	4.87	0.166	4.495
0.166	5.215	0.167	5.17	1.25	5.14	0.25	5.01	0.25	5.018	0.33	4.895	0.75	4.87	0.25	4.495
0.500	5.215	0.183	5.16	1.50	5.14	0.33	5.04	0.50	5.045	0.50	4.890	1.0	4.87	0.50	4.496
0.75	5.215	0.416	5.17	1.583	5.14	0.50	5.07	0.584	5.06	0.75	4.865	1.25	4.887	0.75	4.495
1.00	5.22	0.500	5.16	1.666	5.16	0.583	5.085	0.75	5.07	1.00	4.860	1.5	4.915	1.00	4.465
1.25	5.22	0.584	5.17	2.0	5.21	0.667	5.10	1.0	5.06	1.25	4.89	1.75	4.92	1.5	4.465
1.75	5.215	0.750	5.16	2.5	5.21	1.0	5.10	1.5	5.065	1.5	4.92	1.833	4.92	2.0	4.465
2.00	5.215	0.917	5.15	4.0	5.21	1.25	5.11	2.0	5.065	1.75	4.95	2.00	4.96	2.083	4.495
2.750	5.215	1.085	5.145			2.83	5.11			2.0	4.95	2.66	5.00	2.25	4.495
3.00	5.215	1.500	5.14							2.5	4.95	2.833	5.01	2.33	4.49
4.00	5.215	1.670	5.19							2.75	4.95	3.0	5.01	2.417	4.515
		1.750	5.25							3.0	4.93	3.33	5.015	2.5	4.54
		2.250	5.19							3.5	4.93			2.833	4.535
		4.00	5.195							3.66	4.96			3.5	4.55
		6.00	5.20							4.0	4.95			4.0	4.58
		8.00	5.20							4.25	4.95			5.0	4.6
														6.0	4.625
														10.0	4.58

APPENDIX D (cont'd.)

Tr 24 - 15% Titanium Alloy

701°C		598°C		600°C		500°C		500°C		400°C		Slow heating of transformed 5% Ti specimen	
t	R	t	R	t	R	t	R	t	R	t	R	t	R
0.0	5.62	0.0	5.31	0.0	5.34	0.0	5.17	0.0	5.185	0.0	4.98	201°C	4.1
0.083	5.62	0.083	5.31	0.25	5.34	0.25	5.17	0.25	5.185	0.166		305°C	4.31
0.25	5.62	0.166	5.315	0.33	5.39	0.50	5.17	0.5	5.185	0.33		400°C	4.51
0.500	5.615	0.25	5.315	0.5	5.415	0.75	5.17	0.75	5.185	0.75	4.98	441°C	4.517
0.750	5.615	0.33	5.29	0.583	5.41	1.0	5.17	1.0	5.185	1.0		473°C	4.61
1.50	5.62	0.5	5.35	0.833	5.445	1.166	5.171	1.33	5.189	1.5		500°C	4.685
1.584	5.62	0.75	5.41	1.33	5.51	1.25	5.17	2.0	5.2	1.75		549°C	4.74
1.66	5.63	1.0	5.41	1.75	5.515	1.5	5.18	2.166	5.21	2.0	4.98	600°C	4.81
1.75	5.665	1.5	5.47	2.0	5.515	2.75	5.21	2.33	5.215	2.25	4.985	619°C	4.74
1.833	5.67	2.0	5.49	3.0	5.491	3.0	5.215	2.5	5.22	2.50	5.07	625°C	4.66
2.33	5.69	2.5	5.47	4.0	5.493	3.5	5.225	3.0	5.23	2.833	5.10	630°C	4.65
3.0	5.72	3.0	5.495			3.75	5.23	5.0	5.235	3.0	5.10	650°C	4.715
4.0	5.75	4.0	5.495			4.0	5.231			3.25	5.09	670°C	4.775
5.0	5.77	5.0	5.50			4.25	5.23			3.5	5.09	703°C	4.94
7.0	5.78					4.5	5.235			4.0	5.09	801°C	5.20
8.0	5.78									8.0	5.16	900°C	5.61

APPENDIX E

Micro-hardness Data

Load 100 grams
Duration of impingement 15 seconds
Tr 29 - 5% titanium alloy

Temperature	Duration of Heat Treatment	Hardness No.(DPH) kg/mm.^{2} Average of 10 impressions	Standard Deviation
700°C	15 minutes	197.1	± 4.9
	30 minutes	199.2	± 9.8
	1 hour	196.6	±12.5
	2 hours	199.5	± 8.6
	4 hours	194.2	
	8 hours	208.8	±25.5
	16 hours	204	±13.5
600°C	15 minutes	204.3	±19.5
	30 minutes	194.4	±10.4
	1 hour	212.5	±10
	2 hours	215.4	±13.1
	4 hours	218.8	± 4.5
	8 hours	222.5	±14.2
	16 hours	216.4	±15.8
500°C	15 minutes	224.8	±17.7
	30 minutes	223.6	± 7.4
	1 hour	223.2	±16.7
	2 hours	224.6	±12.8
	4 hours	231.7	±24.8
	8 hours	232.0	±18
	16 hours	219.9	±26.2
400°C	30 minutes	215.2	±12.8
	1 hour	218.3	± 6
	2 hours	224.0	±23.1
	4 hours	234.0	±25.2
	8 hours	235.5	±15.6
	16 hours	236.1	±18.8
300°C	15 minutes	226.7	±14.3
	30 minutes	222.3	±12.6
	1 hour	220.8	±10.7
	2 hours	215.4	±18.6
	4 hours	233.6	±16.7
	8 hours	242.3	±14.6
	16 hours	220.1	±20.1

Appendix E (cont'd.)

Micro-hardness Data

Tr 25 - 15% titanium alloy

Temperature	Duration of Heat Treatment	Hardness No.(DPH) kg/mm.^{2}	Standard deviation
700°C	15 minutes	219.6	± 4.8
	30 minutes	218.5	±14.8
	1 hour	217.4	±11.9
	4 hours	229.5	±13.8
600°C	15 minutes	208.6	± 4.9
	30 minutes	206.5	±10.2
	1 hour	208.8	± 8.7
	2 hours	224.8	± 9
	4 hours	232.0	±10.8
	8 hours	233	±30
500°C	15 minutes	206.5	± 8.4
	30 minutes	215.9	± 8
	1 hour	222.6	±14.5
	2 hours	203.1	±10.3
	4 hours	201.2	± 8.6
	8 hours	199.6	±18.7
	16 hours	239.0	±16.6
	32 hours	229.3	±17.1
400°C	15 minutes	209.1	±11.7
	30 minutes	214.2	±15.6
	1 hour	218.6	±10.1
	2 hours	217.0	± 6
	4 hours	221.8	± 9.3

APPENDIX F

d-Spacings (Angstroms) of Zr-Nb-5% Ti alloy - wire specimens

Index	NBS	After Whitmore 5.6% Ti; 17.6% Nb	Transformed at 600°C 5% Ti; 17.6% Nb
100 α	2.798	2.769	2.751
002 α	2.573	2.540	2.548
101 α	2.459	2.434	2.458
bcc			2.358
102 α	1.894	1.878	1.882
003 α			1.741
bcc			1.665
110 α	1.616	1.606	1.606
103	1.463	1.452	1.460
bcc			1.420
200 α	1.399	1.389	1.390
112 α	1.368	1.361	1.362
201 α	1.350	1.340	1.343
004 α	1.287	1.278	1.276
202 α	1.230	1.221	1.234
113 α			1.172
bcc			1.107
bcc			1.105
203 α	1.084	1.077	1.080
210 α	1.059	1.051	1.052
211 α	1.036	1.029	1.031
114 α	1.006	1.001	1.004
bcc			0.975
105 α	0.966	0.960	0.961
204 α	0.947	0.941	0.944
300 α	0.933	0.928	0.929
213 α	0.900	0.896	0.896
bcc			0.889
302 α	0.877	0.873	0.873
106 α	0.820	0.819	0.825
214 α			0.815
220 α		0.804	0.805
Held at 600°C for ten minutes identified as body-centered cubic phase			2.473 1.734 1.437 1.245 1.114 1.014 0.941) 0.942) 0.831) 0.832) 0.787

BIBLIOGRAPHY

1. Finlayson, M.J., Isothermal Transformation in Eutectoid Zirconium Niobium Alloys, M.A.Sc. Thesis, University of British Columbia (1957).

2. Whitmore, B.C., Zirconium-Rich Corner of the Zirconium-Titanium-Niobium Constitutional Diagram, M.A.Sc. Thesis, University of British Columbia (1958).

3. Lustman, B., and Kerze, F., editors, The Metallurgy of Zirconium, National Nuclear Energy Series, McGraw-Hill (1955).

4. Pfeil, P.C.L., A Critical Review of the Alloying Behaviour of Zirconium, A.E.R.E. - M/TN-11, March 1950.

5. Pfeil, P.C.L., A Discussion of the Factors Affecting the Constitution of Zirconium Alloys, A.E.R.E. M/R 960, June 27, 1952.

6. Domagala, R.F., A Study of the Mechanisms of Heat Treatment of Zirconium Base Alloys, Armour Research Foundation Report for A.E.C., July 17, 1956.

7. Domagala, R.F., Levinson, D.W., and McPherson, D.J., Transformation Kinetics and Mechanical Properties of Zr-Mo Alloys, A.I.M.E. Trans., 209, 1191.

8. Austin, J.B., and Rickett, R.L., A.I.M.E. Trans., 135, 396 (1939).

9. Mishima, T., Hasiguti, R. and Kimura, Y., Proc. First World Met. Conf., A.S.M., 668, (1951).

10. McIntosh, A.B., J. Inst. Metals 85, 1855, April 1957.

11. Anderson, C.T., Hayes, E.T., Roberson, A.H. and Kroll, W.T., A Preliminary Survey of Zirconium Alloys, U.S. Bureau of Mines Investigations, No. 4658.

12. Simcoe, C.R., and Mudge, W.L. Jr., A.E.C. Report No. WAPD-38, November 21, 1951.

13. Keeler, J.H., A.E.C. Report No. SO-2504, January 5, 1952.

14. Litton, F.B., Iron Age, 167, 95-99 and 112-114, (1951).

15. Hodge, E.S., A.E.C. Report No. T 1D-5061, January 31, 1952.

16. Rogers, B.A., and Atkins, D.F., A.I.M.E. Trans. 203, 1034, (1955).

17. Domagala, R.F., and McPherson, D.J., A.I.M.E. Trans. 206, 620 (1956).

18. Bychkov, Yu, F., Rozanov, A.N. and Skorov, D.M., Atomnaya Energiya 2, 146-157, (1957).

19. Fast, J.D., The Transition Point Diagram of the Zirconium-Titanium System, Rec. Trav. Chim., 58, 973 (1939).

Bibliography (cont'd.)

20. Hayes, E.T., Roberson, A.H. and Paasche, O.G., Zirconium-Titanium System, Constitutional Diagram and Properties, U.S. Bureau of Mines Investigations, 4826, November 1951.

21. Hansen, M., Kamen, E.L., Kessler, H.D., and McPherson, D.J., Systems Titanium-Molybdenum and Titanium-Columbium, A.I.M.E. Trans., 191, 881 (1951)

22. Rhines, F.N., Phase Diagrams in Metallurgy, McGraw-Hill, (1956).

23. Schwartz, C.M., and Mallett, M.W., Observations on the Behaviour of Hydrogen in Zirconium, A.S.M. Trans., 46, 640, 1954.

24. Cottrell, A.H., Theoretical Structural Metallurgy, Edward Arnold (1955).

25. McQuillan, M.K., and McQuillan, A.D., Titanium, Chapt. 10, 335, Butterworths Scientific Publications (1956).

26. Polonis, D.H., Butters, R.G., and Parr, J.G., Research 7, No. 2 (1954).

27. Properties of Metallic Surfaces, Inst. Metals, 356, (1953).